



Glacial-interglacial Circumpolar Deep Water temperatures during the last 800,000 years: estimates from a synthesis of bottom water temperature reconstructions

David M. Chandler¹ and Petra M. Langebroek¹

¹NORCE Norwegian Research Centre, Bjerknes Centre for Climate Research, Bergen, Norway

Correspondence: David Chandler (dcha@norcereserch.no)

Abstract. Future climate and sea-level projections depend sensitively on the response of the Antarctic Ice Sheet to ocean-driven melting and the resulting freshwater fluxes into the Southern Ocean. Incursion of Circumpolar Deep Water (CDW) across the Antarctic continental shelf, and into cavities beneath ice shelves, is increasingly recognised as a crucial heat source for ice shelf melt. Quantifying past changes in the temperature of CDW is therefore of great benefit for modelling ice sheet response to past warm climates, for validating paleoclimate models, and for putting recent and projected changes in CDW temperature into context. Here we synthesise the few available bottom water temperature reconstructions representative of CDW and its principal source water mass (North Atlantic Deep Water) over the past 800 kyr. Estimated CDW temperature anomalies consistently reached ca. -2°C during glacial periods, warming to $+0.1$ to $+0.5^{\circ}\text{C}$ during the strongest interglacials (marine isotope stages MIS 11, 9, 5, and 1). The temperature anomaly in MIS 7 was comparatively cooler at ca. -0.6°C . Despite high variance amongst a small number of records, and poor (4 kyr) temporal resolution, we find persistent and close relationships between our estimated CDW temperature and Southern Ocean sea-surface temperature, Antarctic surface air temperature, and global ocean temperature reconstructions at glacial cycle time scales. Given the important role that CDW plays in connecting the world's three main ocean basins, and in driving Antarctic Ice Sheet mass loss, additional temperature reconstructions targeting CDW are urgently needed to increase temporal resolution and to decrease uncertainty in past CDW temperatures – whether for use as a boundary condition, model validation or in their own right.

1 Introduction

In its position at the southern end of the Atlantic meridional overturning circulation (AMOC), the Southern Ocean plays a major role in the Earth's climate. Interactions between the Southern Ocean and Antarctic Ice Sheet drive changes in ice discharge and ocean circulation, which in turn have global-scale impacts on climate (Bronse laer et al., 2018; Rintoul, 2018; Mackie et al., 2020b; Noble et al., 2020). Complex feedbacks between grounded ice dynamics, ice shelves and ocean circulation are either poorly understood and/or difficult to capture at adequate resolution in numerical simulations (Bronse laer et al., 2018; Edwards et al., 2019; Fox-Kemper et al., 2021; Bamber et al., 2022; Siahhan et al., 2022). As a result, the contribution of Antarctica to future sea-level and climate change remains very uncertain (Fox-Kemper et al., 2021; Bamber et al., 2022).



To help inform future climate and sea-level projections, we can reconstruct or simulate past climates, and their corresponding
25 ocean and ice sheet responses, for periods when the Earth was warmer than present. These experiments complement future
projections as they represent climate and ice sheet states outside of those for which direct observations are available (Tzedakis
et al., 2009; Gilford et al., 2020; DeConto et al., 2021). As the most recent warmer period in geological history, the last
interglacial (LIG) has seen widespread interest as an analogue for future warming, from the perspectives of both paleoclimate
(Mercer, 1984; Bakker et al., 2014; Arias et al., 2021; Otto-Bliesner et al., 2021; Zhang et al., 2023) and the resulting ice
30 sheet response (Mercer, 1978; Scherer, 1991; Goelzer et al., 2016; DeConto et al., 2021; Golledge et al., 2021). This interest
likely reflects the relatively greater availability and/or resolution of LIG paleoenvironmental reconstructions, compared to
those for older warm periods. However, there have been many Quaternary interglacials before the LIG, some a little warmer
or cooler than the present (Tzedakis et al., 2009; Yin and Berger, 2015; Past Interglacials Working Group of PAGES, 2016).
Climate and ice sheet simulations through several glacial-interglacial cycles build a much more complete picture of feedbacks,
35 instabilities and tipping points in the Earth system. Of particular interest here is the period after the mid-Pleistocene transition
(MPT, at ca. 1250-700 ka: Clark et al., 2006; Legrain et al., 2023), and particularly marine isotope stages (MIS) 11, 9, 7
and 5, since these best represent the 100-kyr glacial cycles of our pre-industrial interglacial period. However, we should note
that the moderate (SSP2-4.5) and high (SSP5-8.5) IPCC warming scenarios could take us beyond the global surface warming
magnitudes reconstructed in any Quaternary interglacial (IPCC 6th Assessment Report, Technical Summary: Arias et al., 2021).
40 Southern Ocean sea-surface temperature (SST) and sea-ice during the LIG and preceding glacial (the penultimate glacial
maximum, PGM) have been the focus of several recent synthesis studies (Hoffman et al., 2017; Turney et al., 2020; Chandler
and Langebroek, 2021b; Chadwick et al., 2022). Important climatic changes in the Southern Ocean extend far deeper than
the surface waters: the region's role in the AMOC (Buckley and Marshall, 2016; Rintoul, 2018), deep ocean heat storage
(Gjermundsen et al., 2021), and in delivering warm water *at depth* to cavities beneath Antarctic ice shelves (Walker et al.,
45 2007; Wåhlin et al., 2010; Herraiz-Borreguero et al., 2015; Silvano et al., 2017), means that changes in the temperature of deep
water masses are a crucial consideration in both climate and ice sheet simulations. The importance of upwelling circumpolar
deep water (CDW) around Antarctica is being increasingly recognised, as the sensitivity of key Antarctic Ice Sheet sectors to
sub-surface ocean warming becomes clearer (Walker et al., 2007; Herraiz-Borreguero et al., 2015; Silvano et al., 2017; Reese
et al., 2018; Noble et al., 2020; van Wijk et al., 2022).
50 Despite the apparent importance of deep water masses, there is still a strong reliance on surface temperature reconstructions
for evaluating climate models (e.g., Otto-Bliesner et al., 2021; Purich and England, 2021). The bias presumably reflects the
availability of proxy reconstructions, but at the same time there is no guarantee that models selected on the basis of their match
to surface conditions will show similar skill in simulating deeper levels. This is particularly the case in the Southern Ocean,
where processes that are not yet well represented in CMIP models can drive subsurface temperature changes in directions
55 opposite to those at the surface (Rintoul, 2018; Mackie et al., 2020b; Bronselaer et al., 2018). Indeed, a significant difficulty in
simulating Southern Ocean warming, and the Antarctic Ice Sheet response to warming, are the strong ice - ocean - atmosphere
interactions at sub-grid scales (Heywood et al., 2014; Hewitt et al., 2020; Mackie et al., 2020a; Purich and England, 2021).
However, the high computational cost of fully-coupled models limits experiments to short (decadal) time periods (e.g., Kreuzer



et al., 2021; Pelletier et al., 2022; Siahhaan et al., 2022). For now, if we want to adequately resolve important oceanographic or ice flow features, uncoupled or semi-coupled models reliant on imposed or parameterised ice/ocean boundary conditions remain crucial for simulations over centennial to orbital time scales.

Motivated by the need for CDW temperatures as an ocean temperature boundary condition in stand-alone (uncoupled) Antarctic Ice Sheet simulations, this paper synthesises the sparse proxy reconstructions that are available to estimate changes in CDW temperature over the last 800,000 years. This time span is constrained by the period for which there are sufficient data to establish a meaningful synthesis at a practical resolution. Conveniently this period covers the latter part of the Pleistocene dominated by 100 kyr glacial cycles after the MPT (Clark et al., 2006; Legrain et al., 2023), and allows comparison with the full duration of the EPICA Dome C (EDC) ice core record (Jouzel et al., 2007). Besides our original motivation, estimates of past CDW temperature variability are also useful for putting present-day changes into perspective.

2 Modern oceanographic setting

This section provides a very brief overview of the complex Southern Ocean circulation, included here as context for the temperature reconstructions. The cited studies provide much more detail.

CDW comprises the relatively warm water mass and its variants (lower, upper and modified CDW) forming the bulk of the water within the Antarctic Circumpolar Current (ACC). North of the Southern Polar Front, CDW lies at intermediate depths between the underlying colder and saltier Antarctic Bottom Water (AABW), and the overlying colder and fresher surface water masses (Marshall and Speer, 2012; Pardo et al., 2012). South of the Southern Polar Front, upwelling of CDW is driven partly by diverging Ekman transport beneath the mid-latitude westerlies and polar easterlies (Marshall and Speer, 2012; Tamsitt et al., 2021), and partly by topography beneath the ACC (Tamsitt et al., 2017).

Some of the upwelling CDW is subsequently transported southwards onto the Antarctic continental shelf, by a range of processes including eddies, internal waves, dense water outflow, topographic influences, and Ekman transport (Stewart and Thompson, 2015; Tamsitt et al., 2021; Darelius et al., 2023). Mixing with local surface and shelf water masses further transforms CDW temperature and salinity as it crosses the shelf (MacAyeal, 1984; Pardo et al., 2012; Petty et al., 2013). This cross-shelf transport of modified CDW reaches the cavities beneath 'warm' Antarctic ice shelves, including those in the Amundsen Sea Embayment, and those draining the Aurora and Wilkes basins of East Antarctica (Walker et al., 2007; Petty et al., 2013; Silvano et al., 2017; van Wijk et al., 2022). Even modified CDW has sufficient thermal forcing to cause rapid ice shelf basal melting (exceeding 10 m yr^{-1} : Adumusilli et al., 2020) near Antarctic grounding lines. CDW does not currently enter cavities beneath 'cold' ice shelves such as Filchner-Ronne or Ross, except in very localised regions (Darelius et al., 2023). Instead, beneath these 'cold' ice shelves, slower rates of basal melt are driven mainly by high salinity shelf water (HSSW) originating from sea-ice processes (brine rejection) (MacAyeal, 1984; Petty et al., 2013). It is this ocean-driven melting of ice shelves, and its resulting freshwater release, that is a crucial component in Antarctic Ice Sheet models and climate models over a broad range of time scales.



CDW is sourced mainly from southwards flowing North Atlantic Deep Water (NADW) (Sloyan and Rintoul, 2001; Lumpkin and Speer, 2007; Talley, 2013; Tamsitt et al., 2017), but on its path around the ACC it is cooled by mixing with other water masses (e.g., Weddell Sea deep water), particularly in the Scotia Sea (Naveira Garabato et al., 2002). The Indian and Pacific oceans lack overturning circulations equivalent to the AMOC (Broecker et al., 2006; Thompson et al., 2016), and although some Pacific deep water likely enters the ACC west of the Drake Passage, this joins the upper CDW and is returned northwards in Antarctic Intermediate Water (it is mostly the NADW-rich lower CDW that is transported southwards and onto the continental shelf) (Sloyan and Rintoul, 2001; Kawabe and Fujio, 2010; Wählin et al., 2010; Talley, 2013; Biddle et al., 2017; Assmann et al., 2019). Hence, the temperature of CDW accessing ice shelf cavities should reflect the temperature of its dominant precursor water mass (NADW), with an additional cooling signature attributed to subsequent mixing within the ACC and during cross-shelf transport.

3 Methods

3.1 Sites selection

CDW is an elusive water mass for paleotemperature reconstructions. As noted above, CDW lies above AABW, preventing the use of bottom water temperature (BWT) reconstructions from benthic organisms except where the bathymetry penetrates upwards through the AABW and into the CDW (for example, on the Chatham Rise: Elderfield et al., 2012). Meanwhile, CDW (and particularly lower CDW, of greatest consequence for ice shelf melt: Wählin et al., 2010; Biddle et al., 2017; Assmann et al., 2019) lies at depths beyond the reach of proxies based on surface or even sub-surface planktic organisms. Finally, sediments on the Antarctic continental shelf were likely repeatedly overridden by grounded ice during glacial stages and may also be disturbed by deep iceberg keels. Even though suitable BWT proxies are available for the continental shelf (Hillenbrand et al., 2017; Totten et al., 2017; Mawbey et al., 2020), this reworking by icebergs and grounded ice hinders reconstructions representative of CDW directly accessing ice-shelf cavities prior to the Holocene.

The above difficulties are perhaps compounded by the remoteness of the Southern Ocean and a greater community interest in other environmental indicators (e.g., $\delta^{18}\text{O}$, $\delta^{13}\text{C}$, and planktic SST proxies). To-date, at glacial-interglacial timescales there are no reconstructions of CDW temperature from the Antarctic continental shelf, and only two or three sites representing CDW in the Southern Ocean (ODP sites 1123, 1094, possibly 1090: Elderfield et al., 2012; Hasenfratz et al., 2019; Bates et al., 2014, respectively) (Fig. 1). To achieve reasonable statistical confidence and temporal resolution in CDW temperature changes, even at coarse (multi-millennial) time scales, we need to look further afield to the water masses from which CDW is derived, and assume these same water masses and regions have contributed to CDW under past climates. Under that assumption, *changes* in these source-region water temperatures should be representative of *changes* in CDW temperature. This greater scope expands our region of interest to include NADW in its two main source regions (Labrador Sea water; Iceland-Scotland and Denmark Strait overflow waters), and along its transit south in the deep western boundary current which forms the lower, southbound leg of the AMOC (Fig. 1) (Lumpkin and Speer, 2007; Pardo et al., 2012; Rhein et al., 2015; Buckley and Marshall, 2016).



NADW source regions yield the three additional sites Chain 82-24-4PC (Cronin et al., 2000), DSDP 607 and ODP 980 (Bates et al., 2014). The deep western boundary current is represented by just one relevant site (MD07-3076Q: Roberts et al., 2016) covering the period 20 to 2 ka, which we have not included as it only covers the last deglaciation. Finally, site M16772 (Martin et al., 2002) in the eastern tropical Atlantic lies neither in a NADW source region nor directly within its primary southwards transport pathway, but we include this site as it lies in NADW transported eastwards from the deep western boundary current via an equatorial plume (Smethie et al., 2000; Rhein et al., 2015) (Fig. 1).

As noted above (Section 2), Pacific deep water is unlikely to make an important contribution to lower CDW and we therefore exclude one site in the eastern tropical Pacific (TR163-31P: Martin et al., 2002).

Given the wide geographic scope that extends well beyond the boundaries of CDW, we are effectively compiling a BWT synthesis, rather than directly a CDW temperature synthesis. We reiterate here that we use this approach to infer *changes* in CDW temperature (i.e., anomalies from present-day conditions), rather than estimating CDW temperatures directly. This point is discussed further in Sections 5.2 and 5.3.

3.2 Bottom water temperature synthesis

In total we use seven sites located as described above (6 Atlantic, 1 SW Pacific: Table 1, Fig. 1). BWT at these sites has been reconstructed using benthic foraminiferal $\delta^{18}\text{O}$ and Mg/Ca, and ostracod Mg/Ca. The records are published at varying temporal resolution, using different calibrations and chronologies. Therefore, to improve consistency and to considerably reduce variance, we stacked the records following a similar methodology to that employed in a SST synthesis covering the last 200 ka (Chandler and Langebroek, 2021b). Briefly there are five main steps:

1. Temperatures derived from Mg/Ca were recalculated using recently published calibrations appropriate for that species (see details in the Table 1 caption).
2. The reconstructed 'modern' temperature was subtracted so that down-core temperatures are anomalies from the recent past. Considering the low resolution of the records, the 'modern' temperature is an average of all samples younger than 2 ka (if possible) or otherwise the observed bottom water temperature reported by the original authors.
3. For records with published benthic foraminiferal $\delta^{18}\text{O}$, age models were aligned with the Lisiecki and Raymo (2005) LR04 global benthic stack.
4. All records were resampled to 4 kyr resolution following the method used by Chandler and Langebroek (2021b). This choice of coarse resolution reflects a necessary compromise between data resolution and uncertainty, because the uncertainty increases as resolution increases (due to fewer contributing sites). Note that our method admits gaps: we do not interpolate low-resolution records onto a higher resolution time series.
5. Uncertainties for each time slice were calculated using the t-distribution, under the assumption that temperatures at each site are sampled independently from those at other sites.

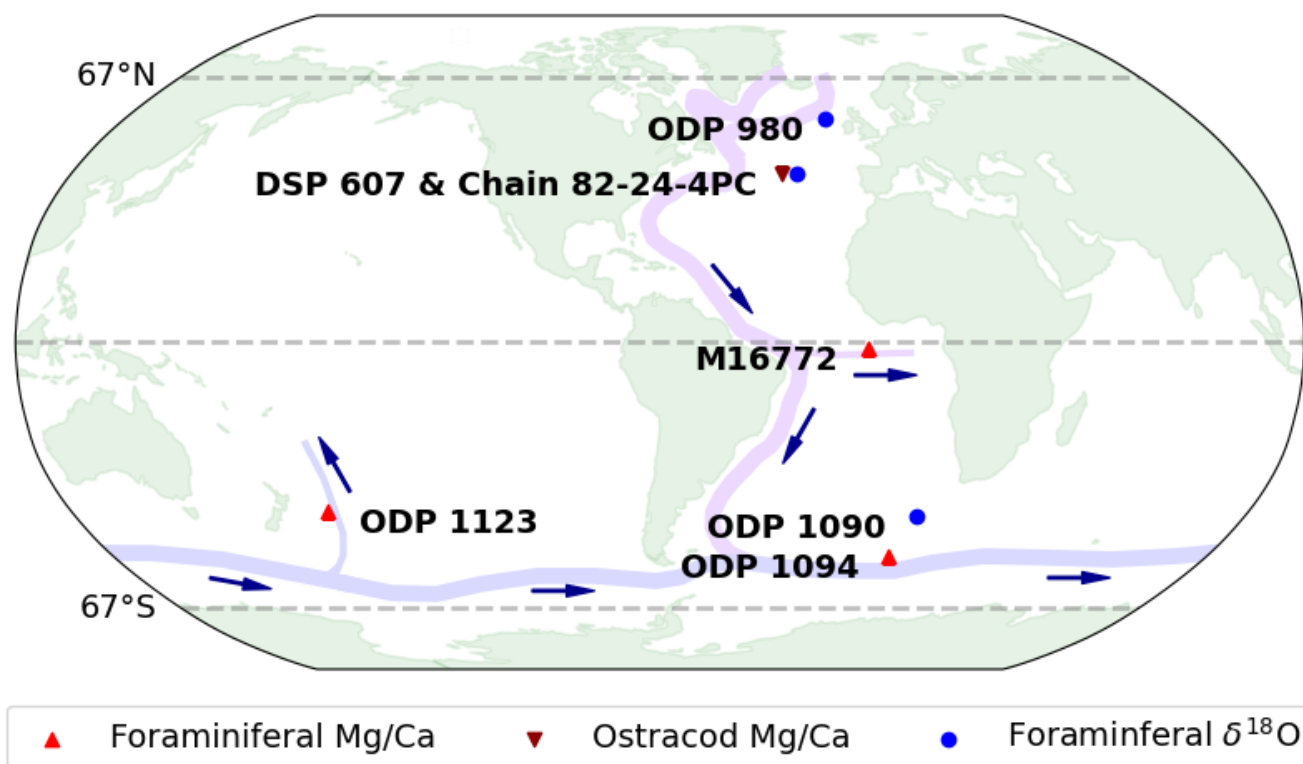


Figure 1. Locations of marine sediment cores used in the synthesis. Additional details of each site are provided in Table 1. Also shown is a simplified, schematic representation of the main pathways for southbound NADW (purple) and eastbound CDW (blue), based on Smethie et al. (2000), Oppo and Curry (2012) and Rhein et al. (2015). Sites ODP 980, DSP 607 and Chain 82-24-4PC lie in NADW close to its North Atlantic source regions. Site M16772 lies in an eastwards heading plume of NADW that breaks off the deep western boundary current. Site ODP 1090 lies close to the boundary of NADW and CDW in the South Atlantic, site ODP 1094 lies in CDW within the Antarctic Circumpolar Current (ACC), and site ODP 1123 lies in CDW that branches north from the main ACC in the SW Pacific.

4 Results

155 Each of the 4-kyr time slices from 800 ka to present has BWT contributions from at least 3 sites (Fig. 2). The record shows clear glacial-interglacial cycles consistent with many other relevant proxy records (e.g., Fig. 3), but we note that high uncertainties prevent detailed quantitative comparison of the magnitudes of BWT warming in specific interglacials. Cooling is similar through each glacial, typically close to -2°C (again, bearing in mind the wide uncertainties). Prior to MIS 11 it is unclear whether the reduced amplitude of glacial-interglacial cycles is a genuine feature (consistent with weaker interglacials in the

160 Antarctic surface air temperature record, Fig. 3), or an artefact of the greater inter-site variance which tends to smooth out peaks.



We observe some systematic biases in reconstructed BWTs between the two main proxies ($\delta^{18}\text{O}$ vs Mg/Ca) and between the two water masses (NADW vs CDW) (Fig. 4). The mean Mg/Ca BWT anomaly is on average 0.5°C warmer than the mean $\delta^{18}\text{O}$ anomaly, and varies over a wider range. The warm bias is particularly noticeable in Fig. 2 during interglacials, which show warmer peaks in the Mg/Ca BWT than in the $\delta^{18}\text{O}$ BWT. When comparing the two water masses, we find BWT anomalies at sites currently situated in CDW are on average 0.6°C warmer than those situated in NADW. In both comparisons the correlations are well scattered, but are surprisingly stronger for NADW vs CDW ($r^2 = 0.31$) than for $\delta^{18}\text{O}$ vs Mg/Ca ($r^2 = 0.23$). Both proxies contributed reconstructions in both water masses, and unfortunately these potentially interesting differences cannot yet be analysed in detail with only 7 sites in total.

Comparing our synthesis with other Southern Hemisphere paleotemperature reconstructions, we find BWT is well correlated with both Southern Ocean SST and Antarctic surface air temperature (Fig. 5) at 4 kyr time scales, but the amplitudes of glacial-interglacial BWT changes are weaker, reaching about 50% and 20% of the respective changes in SST and Antarctic surface air temperature. At global scale our BWT is also well correlated with a global mean deep water temperature (GDWT) reconstruction by Rohling et al. (2021), and the magnitudes are very closely matched through most of the study period (Fig. 3) – but in this case the apparently weaker changes in BWT than in GDWT (Fig. 5) are mainly due to a slight offset in the timing of interglacial peaks.

The coarse temporal resolution hinders detailed analysis of leads/lags between BWT and other records, that we might otherwise use to evaluate whether deep ocean temperatures are driven by surface climatic changes or vice-versa. However, we can at least suggest there is likely to be less than 4 kyr lead/lag between BWT and either Antarctic surface air temperature or Southern Ocean SST, as the peaks in correlation coefficients are centred near zero lag (Fig. 6a,b). In contrast it is likely that BWT lags global mean deep water temperature (Rohling et al., 2021) by close to 4 kyr (Fig. 6c).

5 Discussion

Considering the vast distances (109 degrees of latitude) separating the seven sites, and the different proxies employed, there is not surprisingly some considerable variance between BWT anomalies at different sites. The combination of high variance and a low number of sites, particularly in the period before ca. 300 ka, yields wide uncertainties for many of the time slices (Fig. 2). Besides uncertainty arising from geographic variability, this variance could reflect non-thermal influences on Mg/Ca paleothermometry (especially at relatively cold temperatures, e.g., Raitzsch et al., 2008; Stirpe et al., 2021), and uncertainties in sea-level estimates and transfer functions required in the oxygen isotopic reconstructions (Siddall et al., 2010; Bates et al., 2014). See the original studies cited in Table 1, and Section 5.2 below, for further discussion of assumptions and errors.

The original motivation of this study was to estimate changes in CDW temperature through recent glacial-interglacial cycles. Our approach of including temperature reconstructions from the distant North Atlantic is not immediately intuitive and was justified only on its modern oceanographic basis (Section 2). Reasonable correlation between the reconstructed NADW and CDW temperatures (Fig. 4) empirically supports our approach. The mean 0.6°C bias between the NADW and CDW temperature anomalies is considerably smaller than the $\sim 3^\circ\text{C}$ glacial-interglacial variability. However, since ice shelf basal melting

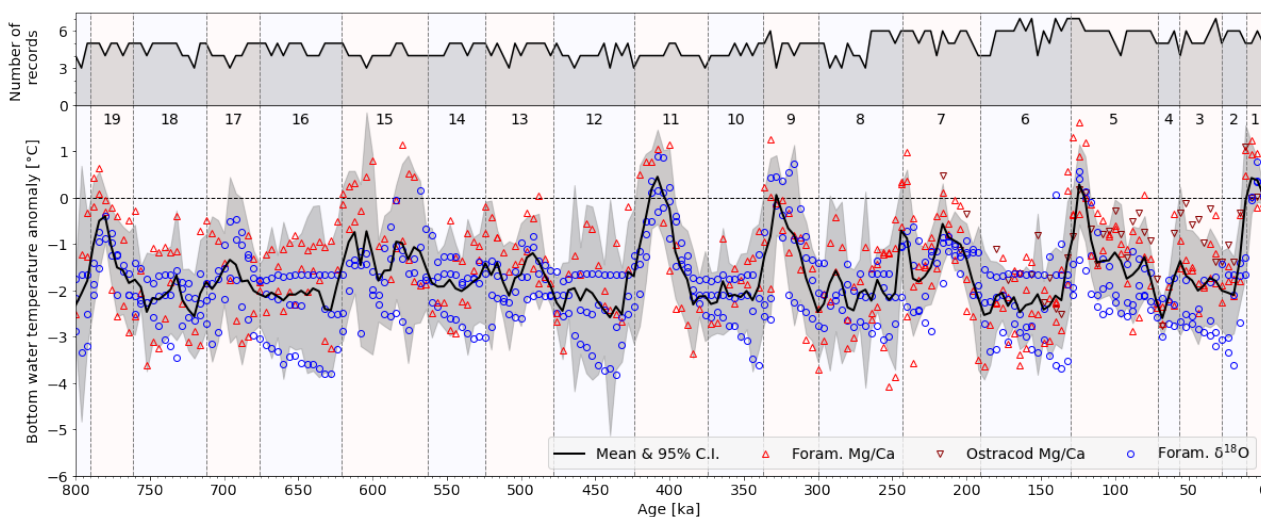


Figure 2. Time series of revised bottom water temperature anomalies at the seven sites in Table 1. Following our method in Section 3.2, records have been resampled to 4 kyr resolution, and the 95% confidence interval (shaded grey) is calculated using the t distribution. Numbers and vertical shading show the marine isotope stages (Lisiecki and Raymo, 2005).

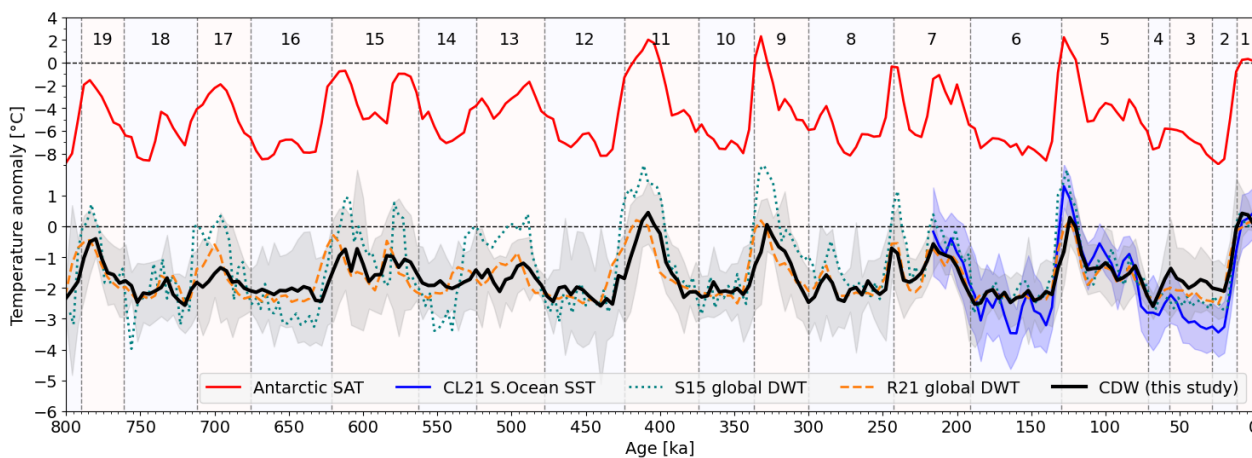


Figure 3. Comparison of CDW temperatures estimated in our BWT synthesis (black with grey shaded 95% confidence interval), with other paleotemperature records: East Antarctic Ice Sheet surface air temp (SAT) from Jouzel et al. (2007) and Parrenin et al. (2013) (red); Southern Ocean SST from Chandler and Langebroek (2021b) (blue with shaded 95% confidence interval); global mean deep water temperature from Shakun et al. (2015) (turquoise dots); and global mean deep water temperature from Rohling et al. (2021) (orange dashes). All records have been resampled to 4 kyr to match the resolution of our BWT synthesis, except for Shakun et al. (2015) which is plotted at its original 3 kyr resolution.

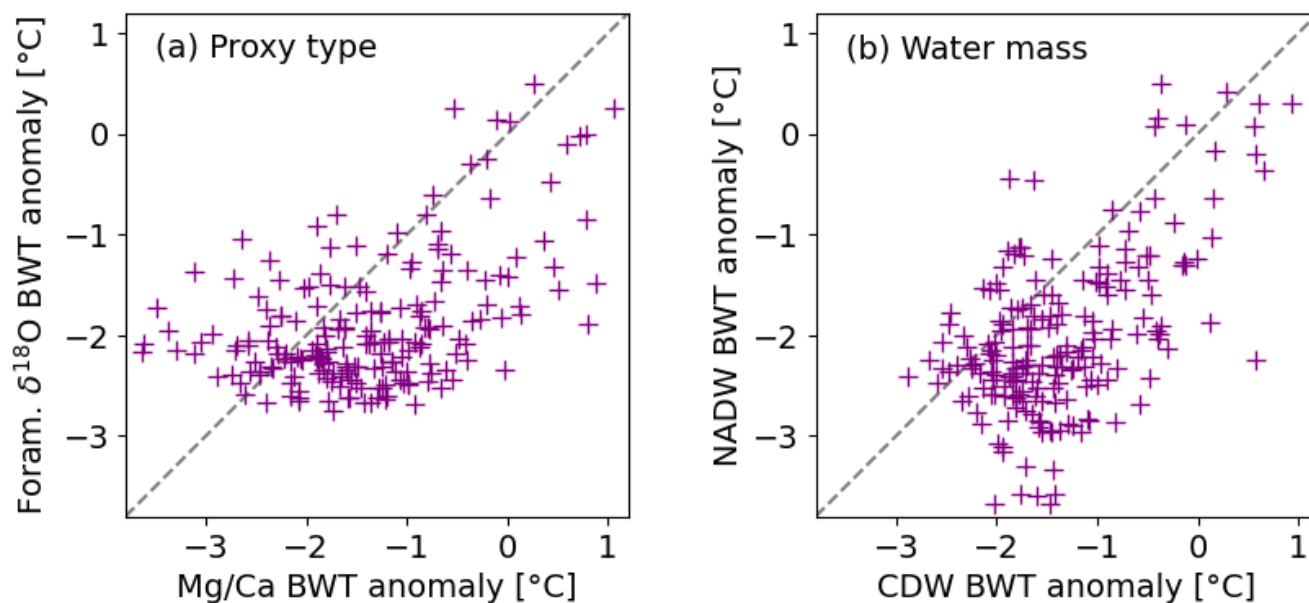


Figure 4. Correlation between (a) BWT reconstructed with Mg/Ca and BWT reconstructed with foraminiferal $\delta^{18}\text{O}$; and (b) BWT at sites situated in CDW and sites situated in NADW under present-day conditions. Dashed lines indicate the 1:1 ratio.

195 is very sensitive to ocean temperature, this bias is relatively important; there is also the question of changes in NADW contribution to CDW under glacial climates (Section 5.3 below). As more data become available for the Southern Ocean we would recommend eventually excluding the NADW sites from CDW temperature estimates, and instead focusing on a comparison of the individual changes in these two important water masses.

Weaker correlation between the two proxy groups, than between the two water masses (Fig. 4), is indicative (tentatively, 200 for only 7 sites) that methodological uncertainties remain an important – probably greatest – contributor to the wide scatter in individual time slices. These are described further below (Section 5.2). Similar to the recommendation in our Southern Ocean SST synthesis (Chandler and Langebroek, 2021b), this should underline the caution required when interpreting temperature reconstructions based on a single site or proxy in this region.

5.1 Comparison with other temperature records

205 Despite the wide uncertainties, strong relationships emerge between our CDW temperature estimates and other paleotemperature records for the Southern Hemisphere and even globally (Figs. 3, 5). Indeed, the correlations of the CDW temperature with Antarctic surface air temperature, Southern Ocean SST and global mean deep water temperature (DWT) (r^2 values 0.70, 0.72 and 0.64, respectively) are stronger than correlations between the two BWT proxies ($r^2 = 0.23$) or between NADW and CDW ($r^2 = 0.31$) (Fig. 4). Such strong relationships between temperature records are encouraging as they indicate persistence 210 of key underlying drivers of the climate system throughout the study period (800 ka to present), supporting the notion that

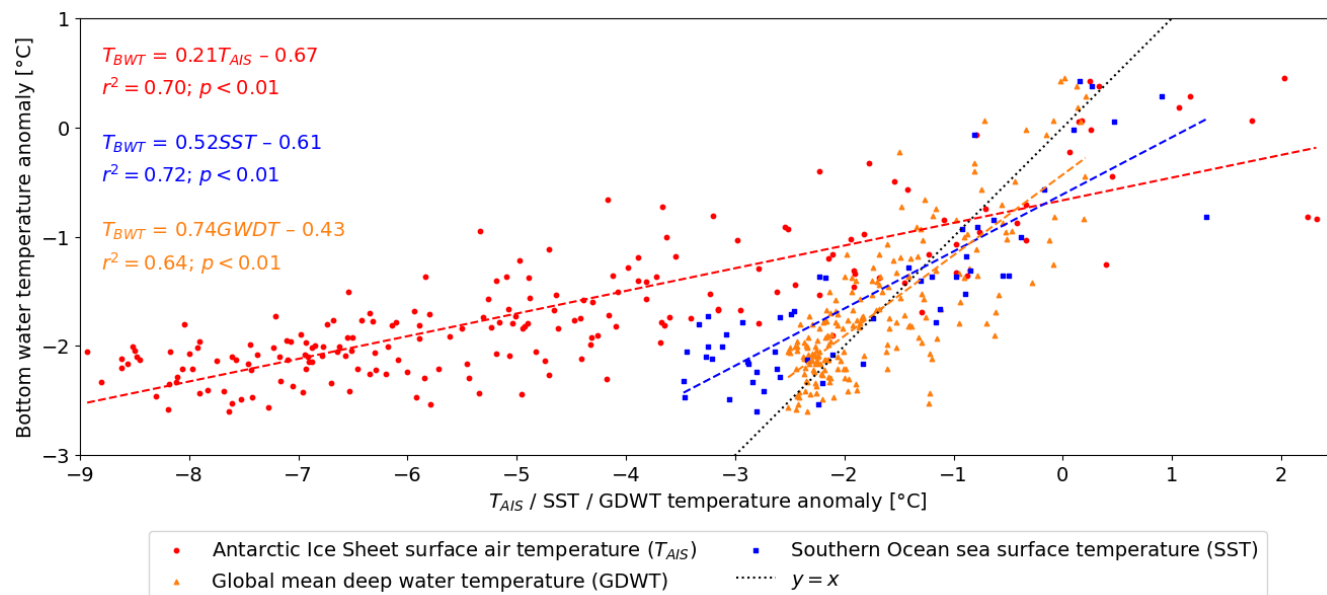


Figure 5. Correlation between our BWT synthesis (y-axis) and other paleotemperature records (x-axis): these are Antarctic Ice Sheet surface air temperature from 800 ka to present (T_{AIS} ; red) (Jouzel et al., 2007; Parrenin et al., 2013), Southern Ocean sea surface temperature from 220 ka to present (SST; blue) (Chandler and Langebroek, 2021b), and global mean deep water temperature (GDWT, orange) (Rohling et al., 2021). All records have been resampled to 4 kyr to match our BWT synthesis.

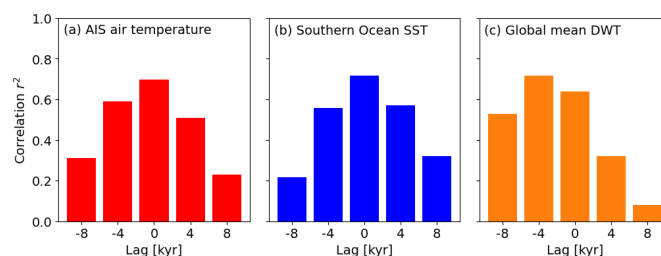


Figure 6. Correlation between our BWT synthesis and other paleotemperature records, after introducing a lag of -8 to +8 kyr in the BWT record. A negative lag indicates that changes in the other record precede changes in BWT. The three panels are the Antarctic Ice Sheet surface air temperature (panel a) (Jouzel et al., 2007; Parrenin et al., 2013); the Southern Ocean sea surface temperature (panel b) for the period 220 ka to present (Chandler and Langebroek, 2021b); and the global mean deep water temperature (panel c) (Rohling et al., 2021). Since the BWT time series is at 4 kyr resolution, leads/lags shorter than 4 kyr cannot yet be evaluated.

paleoenvironmental reconstructions from any one or several glacial cycles within this period can provide valuable insights into our present-day interglacial climate.

There are several features in our synthesis which may not yet be statistically significant themselves, but which do match patterns in many other records. Specifically, we make comparisons with global DWT records based on (i) paired SST and planktic



215 $\delta^{18}O$ records mostly outside of NADW/CDW source regions Shakun et al. (2015) and (ii) reanalysis of the global benthic $\delta^{18}O$
stack (Rohling et al., 2021); our 220 ka Southern Ocean SST synthesis based on planktic proxies Chandler and Langebroek
(2021b); a 20 ka high-resolution NADW temperature record from the South Atlantic, based on benthic foraminiferal Mg/Ca
(Roberts et al., 2016); and an estimate of mean ocean temperature from 157 to 120 ka using ice core noble gas ratios (Shackle-
ton et al., 2020). We also make comparisons with surface air temperatures estimated using ice core stable water isotopes: these
220 are from a five-site average in East Antarctica (Parrenin et al., 2013); the WAIS Divide ice core in West Antarctica (Cuffey
et al., 2016), and the GRIP ice core in central Greenland (Johnsen et al., 1995). Comparing these records allows us to highlight
the following three important common features.

The first common feature is the early Holocene thermal maximum, as recognised in a diverse range of temperature recon-
structions from both hemispheres (e.g., Marcott et al., 2013). The event was captured in this synthesis (albeit coarsely), in the
225 higher resolution SW Atlantic NADW temperature record (Roberts et al., 2016), in both annual and summer Southern Ocean
SST syntheses (Chandler and Langebroek, 2021b), in global mean SST and in one of the global DWT reconstructions (Shakun
et al., 2015), in the East Antarctic and Greenland surface air temperatures (Johnsen et al., 1995; Parrenin et al., 2013), and a
little later (ca. 4 ka) at the WAIS divide (Cuffey et al., 2016).

The second feature is the relatively stronger peaks of interglacials MIS 11, 9 and 5 compared to MIS 7, in our CDW tem-
230 perature estimate, in global DWT (Shakun et al., 2015; Rohling et al., 2021), and in East Antarctica air temperature (Parrenin
et al., 2013). These three interglacials also yielded the highest global mean sea-level in the recent reanalysis of the Lisiecki and
Raymo (2005) (LR04) benthic stack by Rohling et al. (2021).

Third is the consistency in DWT estimates through the last two glacial cycles (Fig. 3). We see relatively steady temperature
anomalies of ca. $-2^{\circ}C$ throughout the penultimate glacial (MIS 6) in our study, in global DWT (Shakun et al., 2015; Rohling
235 et al., 2021) and in mean ocean temperature (Shackleton et al., 2020). This was followed by global deep and mean ocean
temperature warming to ca. $+1^{\circ}C$ during the LIG (Shakun et al., 2015; Shackleton et al., 2020; Rohling et al., 2021, before
resampling to 4 kyr). LIG warming is weaker ($+0.3\pm 0.9^{\circ}C$) in our BWT synthesis at 4 kyr resolution, but can be better
resolved to $+0.8\pm 0.7^{\circ}C$ if running the synthesis at 2 kyr resolution (figure not shown: this is one of the few periods for which
higher resolution reduces uncertainty). Consistent trends are then observed through MIS 5 to 2 in DWT and estimated CDW
240 temperature. Hence, several deep ocean temperature estimates are closely consistent through the penultimate glacial cycle.

Overall our estimated changes in CDW temperature are remarkably similar to the changes in global mean DWT (Rohling
et al., 2021, resampled to 4 kyr) (Fig. 3) throughout the last 800 kyr. The only difference of note is the phase in some cy-
cles (earlier peak in global DWT than in CDW temperature). This would be an interesting aspect to pursue when the CDW
temperatures can be better resolved.

245 The consistencies highlighted above further support both the strength and persistence of coupling between these different
parts of the Earth system over multiple glacial cycles, at least at multi-millennial time scales.



5.2 Uncertainties and limitations

The relatively small variations in BWT over glacial-interglacial cycles have been recognised as a potential challenge in reconstructions (Tisserand et al., 2013; Stirpe et al., 2021). From an optimistic perspective we could see this lower variability as advantageous, since the less an environmental variable changes with time, the less concerned we need to be with reconstructing its changes. However, when considering the high sensitivity of ice shelf basal melt to small temperature changes (e.g. Burgard et al., 2022), we do indeed need accurate estimates of past CDW temperatures - even if these changes have been $< 1^{\circ}\text{C}$.

Compared to planktic organisms used in SST reconstructions, benthic organisms are not subject to lateral advection while sinking, or to strong seasonality, or to varying habitat depth along a temperature gradient within the mixed layer and thermocline (Chandler and Langebroek, 2021a, and references therein). Nevertheless, some of the same problems do still apply – most notably related to seawater chemistry, diagenetic alteration (calcite dissolution, secondary calcite precipitation), and sediment reworking. Additional sources of uncertainty are associated with oxygen isotopic BWT estimates (Siddall et al., 2010; Bates et al., 2014). These error sources are summarised briefly in the sub-sections below, but for more detailed discussion relevant to the specific sites and proxies used in this synthesis please refer to the original publications (Cronin et al., 2000; Martin et al., 2002; Elderfield et al., 2012; Bates et al., 2014; Hasenfratz et al., 2019) and calibrations (Healey et al., 2008; Farmer et al., 2012; Stirpe et al., 2021).

All the records used here are additionally subject to uncertainty in their ages, which can reach several kyr once outside the range of ^{14}C dating. Dating uncertainty can arise from low resolution (due to low sedimentation rate), regional hydrographic variability when compared with global stacks used for alignment, subjective choice of tie-points, and uncertainties in the target chronology.

As more records become available, site-specific assessments of the likely error sources would be worthwhile as an extra quality control step. Given the sparse data available at present we do not discriminate on this basis, or impose any weighting. Instead we assume the associated errors mainly contribute higher variance, rather than a substantial temperature bias, in a synthesis that averages across multiple proxies and oceanographic sedimentary settings. As noted in Section 4 above, comparison of the two proxy groups (Mg/Ca and $\delta^{18}\text{O}$) in Fig. 4 shows substantial scatter indicative of methodological differences that need further investigation when more sites are available or, ideally, when Mg/Ca and $\delta^{18}\text{O}$ temperature estimates are obtained for the same core samples.

5.2.1 Seawater chemistry influences on calcite Mg/Ca

Seawater chemistry affects calcite Mg/Ca mainly through the influence of seawater or pore-water carbonate ion saturation ($\Delta[\text{CO}_3^{2-}]$), which is considered a secondary control on Mg/Ca (especially at cold temperatures) in some foraminifera species (Raitzsch et al., 2008; Tisserand et al., 2013; Stirpe et al., 2021) or possibly a primary control in *Cibicidoides wuellerstorfi* (Yu and Elderfield, 2008). Corrections for this influence are feasible for some species (e.g. Healey et al., 2008) but only if $\Delta[\text{CO}_3^{2-}]$ can also be reconstructed (which can be done in principle from B/Ca: Yu et al., 2008). Records used in this synthesis have not been corrected for $\Delta[\text{CO}_3^{2-}]$; this should be considered in future studies if sufficient data are available. Alternatively, the Mg/Li



280 ratio may in future provide estimates of temperature that are independent of carbonate saturation (Bryan and Marchitto, 2008).
Ostracod Mg/Ca appears less sensitive to $\Delta[\text{CO}_3^{2-}]$ (Farmer et al., 2012) but unfortunately the single relevant reconstruction
available for this synthesis extends back only to MIS 7 (Cronin et al., 2000).

Changes in ambient seawater Mg/Ca ratio are potentially important at Myr timescales (Ries, 2010). However, seawater
Mg/Ca has increased by only ~ 0.1 mol/mol/Myr during the last 20 Myr, towards its modern ratio of ~ 5 mol/mol (Coggon
285 et al., 2010; Evans and Müller, 2012), so that changes in seawater Mg/Ca are not considered important for the purposes of this
study.

5.2.2 Diagenetic alteration, transport, and sample analysis

Post-depositional dissolution or precipitation of calcite can further modify the Mg content of foraminiferal calcite (Sexton
et al., 2006). Dissolution of calcite into seawater or interstitial pore waters with low $\Delta[\text{CO}_3^{2-}]$ biases the isotopic or trace
290 metal content of the remaining shell, while secondary calcite precipitates deposited onto shells from ambient water may have
different isotopic or trace metal signatures to those of the original biomineralised calcite (Broecker et al., 2006; Stirpe et al.,
2021).

Bioturbation causes vertical mixing of foraminifera shells in surface sediments, leading to observed age differences as high
as 1 to 3 kyr between different foraminifera species in the same sediment horizon (Anderson, 2001; Broecker et al., 2006;
295 Mekik, 2014; Ausín et al., 2019). This vertical mixing is equivalent to temporal smoothing of the reconstructed temperature
signal, and most strongly affects sites with lower sedimentation rates. Although bioturbation could be problematic if revising
this synthesis to a higher temporal resolution in future when more data are available, we would not expect this error source to
substantially alter our results at 4 kyr resolution. Reworking for example by winnowing and re-deposition adds a further source
of error to both the reconstructed temperature and the age model, as local sediments become contaminated with older material
300 from distal sites (e.g., Dezileau et al., 2000).

In Mg/Ca paleothermometry the reductive sample cleaning method can cause preferential leaching of Mg, relative to the
oxidative method (Yu et al., 2007; Yu and Elderfield, 2008), as is also the case for planktic foraminifera (Barker et al., 2003).

5.2.3 Sea-level transfer functions for oxygen isotopic bottom water temperature estimates

Benthic foraminiferal calcite $\delta^{18}\text{O}$ depends on both the temperature and $\delta^{18}\text{O}$ of ambient seawater. At glacial cycle timescales,
305 the latter varies primarily with global ice volume, as ^{16}O becomes preferentially locked up in ice sheets so that seawater $\delta^{18}\text{O}$
becomes more positive.

Deconvolving the temperature and seawater $\delta^{18}\text{O}$ contributions requires firstly estimates of global sea-level, secondly a
suitable scaling to convert changes in sea level to changes in seawater $\delta^{18}\text{O}$, and finally a suitable paleotemperature equation
linking benthic calcite $\delta^{18}\text{O}$, water temperature, and seawater $\delta^{18}\text{O}$ (Waelbroeck et al., 2002; Siddall et al., 2010; Bates et al.,
310 2014). Many assumptions are required in each stage, as discussed in detail by these authors. Overall, Bates et al. (2014)
considered this method most appropriate for glacial cycle time scales after the mid-Pleistocene transition (MPT), and less so
for rapid changes during glacial inception or termination, or prior to the MPT. Hence, we consider this method appropriate at 4



kyr time scales in the last 800 kyr. At higher temporal resolutions, the original temperature estimates using this method might benefit from revision using additional sea-level and hydrographic reconstructions that have been published in the last ca. 10
315 years.

A further point of caution is the lack of independence from sea-level records: this is not itself a problem for temperature reconstructions but it should be borne in mind when comparing the reconstructed temperatures with sea-level records (some correlation should be inevitable).

5.3 Persistence of target water masses at selected sites

320 In Section 2 we provided a brief overview of the present-day distribution of CDW and its source regions, that we use as a basis for site selection. Under climates that are increasingly different from present, the question of changes in ocean circulation becomes increasingly important as selected sites may no longer represent the target water mass. Of particular relevance is the debate concerning weakening of the AMOC during glacial climates, based on several proxies including foraminiferal carbon and neodymium isotopic signatures (^{13}C and ϵ_{Nd} , respectively), foraminiferal Cd/Ca and Zn/Ca, and $^{231}\text{Pa}/^{230}\text{Th}$ (e.g.
325 Duplessy et al., 1988; Raymo et al., 1990; Yu et al., 1996; Marchitto et al., 2002; Lund et al., 2011; Kim et al., 2021; Williams et al., 2021). The debate is further addressed in modelling studies (e.g. Rahmstorf, 1994; Gu et al., 2017; Kageyama et al., 2021; Muglia and Schmittner, 2021). With a weaker AMOC, the southbound flow of NADW is thought to have been confined to shallower depths, and underlain by AABW extending further north than its present extent. That could have resulted in some deep Atlantic core sites being bathed in colder AABW, instead of NADW, during glacial climates. It is also possible that
330 NADW was replaced to some extent by a different glacial water mass (glacial North Atlantic intermediate water: GNAIW Boyle and Keigwin, 1987; Duplessy et al., 1988; Marchitto et al., 2002).

The drivers of this change in circulation could have been in the North Atlantic, where changes in sea-ice formation modify deep convection and deep water formation, and/or in the Southern Ocean, where changes in stratification reduced the mixing between Southern Ocean and Atlantic water masses (Duplessy et al., 1988; Muschitiello et al., 2019; Sun et al., 2020; Williams
335 et al., 2021). Either way, the effect of this change in circulation on our CDW temperature estimates may be less marked than might first be anticipated. In the case that shoaling of NADW leads to a switch from NADW to AABW bathing a core site, proxies based on benthic organisms should record a corresponding drop in temperature as AABW is colder than NADW (under present-day conditions). At the same time, recalling that CDW comprises a mix of NADW and colder locally-sourced water masses (Section 2), we would expect the reduced contribution of NADW to CDW to increase the relative importance of the
340 mixing of CDW with colder water masses in the ACC. This change in balance would result in cooling of the CDW, which at least is qualitatively consistent with cooling in the proxy record. Overall, we would anticipate that reconstructed Atlantic BWT cooling caused by a change in water mass should still reflect (albeit less directly) a cooling of CDW in the Southern Ocean. As more reconstructions become available, it would of course be preferable to constrain the temperature changes separately in NADW, CDW and AABW, by combining paleotemperature proxies and water mass tracers employed in sediment cores
345 simultaneously.



5.4 Recommendations for use as a boundary condition or for model validation

As an ocean temperature boundary condition for calculating ice shelf basal melt in an Antarctic Ice Sheet model, this record currently has insufficient temporal resolution to capture rapid temperature changes during interglacial periods, and its uncertainties are likely too large, to be used directly. A 1-dimensional time series also contains no information on spatial variability
350 between ice shelves or even between the Atlantic, Indian and Pacific sectors. Until the uncertainty can be reduced with the addition of further reconstructions, the synthesis would be more appropriately used to complement or validate alternative (less direct) estimates of CDW temperature changes such as those previously employed by paleo ice sheet modellers (Pollard and DeConto, 2012; Tigchelaar et al., 2018; Sutter et al., 2019; Albrecht et al., 2020).

We also note that changes in CDW temperature do not necessarily correlate directly with changes in basal melting: ocean-
355 ice heat transport and sub-shelf melting depend not only on the open-ocean CDW temperature but also the rate of transport of CDW across the continental shelf. Neither the strength of cross-continental-shelf transport of CDW, nor its mixing with other local water masses, can yet be reconstructed directly for any ice shelf in existing proxy records prior to the Holocene. However, the extent to which CDW can access sub-shelf cavities has been parameterised, for example using local geometric factors (DeConto and Pollard, 2016).

360 One of the main uncertainties in our synthesis is the possible switch from NADW to AABW at some core sites during cooler climates. From an ice sheet modelling perspective this issue is likely of little consequence: as the ocean cools below present-day conditions, we would expect basal melting to rapidly decrease, leading to an advance of ice shelf fronts and grounding lines, and an increase in the relative contribution of calving to ice sheet mass balance. If modelling ice sheet response to warming in past interglacials (which is a more common aim of such experiments), the persistent and close relationship between our BWT
365 synthesis and other temperature estimates (Fig. 5 and Section 5.1) supports interglacial ocean circulation patterns similar to that of our modern circulation; in this case our BWT synthesis should provide a good estimate of CDW changes. Under those conditions, the greatest unconstrained uncertainty might be the influence of West Antarctic Ice Sheet collapse on Southern Ocean circulation: this would open deep pathways connecting the Amundsen, Ross and Weddell seas which could substantially impact Southern Ocean circulation (Bougamont et al., 2007; Vaughan et al., 2011).

370 5.5 Priorities for future reconstructions

Given the high value that CDW temperature reconstructions have for ice sheet and climate modellers, whether for model validation or as a boundary condition, further efforts to improve the resolution, reduce variance and add regional variability would be very welcome. These could be addressed by:

1. Analysis of foraminiferal Mg/Ca in additional sediment cores, targeted at sites in the Southern Ocean or South Atlantic.
375 Even relatively low-resolution records, which might have limited use individually, can be helpful in a synthesis of reconstructions provided reasonable age control can be established. This is because we use the t-distribution to calculate confidence intervals, and the width of confidence intervals decreases rapidly with increasing sample size, when sample size is small.



2. Further work to account for the influence on non-thermal factors in Mg/Ca paleothermometry, in particular carbonate
380 chemistry, and how these might be corrected for (Bryan and Marchitto, 2008; Healey et al., 2008; Raitzsch et al., 2008).
3. Application of additional proxies, in particular clumped isotope paleothermometry as this proxy is independent of sea-
water chemistry (e.g. Tripathi et al., 2010; Piasecki et al., 2019). An increased diversity in proxy types helps reduce bias
associated with a single method or organism.
4. Application of multiple proxies to the same core samples would be greatly beneficial, to quantify proxy biases and
385 uncertainties independently of variance contributed by dating uncertainties and geographic variability.

6 Conclusions

Here we have synthesised BWT reconstructions in the Southern Ocean and Atlantic Ocean with the aim of estimating changes in CDW temperature during the last 8 glacial-interglacial cycles (800 ka / MIS 19 to present). Although BWT reconstructions are sparse in comparison to SST, there are sufficient data to establish a statistically meaningful synthesis at 4 kyr resolution.
390 This yields estimated CDW temperature anomalies of ca. -2° during glacial periods, warming to $+0.1$ to $+0.5^{\circ}\text{C}$ during the strongest interglacials (MIS 11, 9, 5, 1) (Fig. 2). The MIS 7 CDW temperature anomaly was comparatively cooler at -0.6° . A warmer early Holocene is consistent with many other paleotemperature records (Section 5.1) but not yet statistically significant owing to the small sample size.

There are many periods of high uncertainty, particularly prior to MIS 11, and the signal-to-noise ratio is generally much
395 poorer than for our recent Southern Ocean SST synthesis that followed a similar approach (Chandler and Langebroek, 2021b). The high variance is likely dominated by methodological rather than geographic variability (see Section 5). Despite the uncertainty, we find strong correlation with the AIS surface air temperature and Southern Ocean SST at time-scales of 4 kyr and longer, with little evidence of substantial leads/lags (Figs. 3, 5, 6). We also find very close agreement between our CDW temperature estimates and the Rohling et al. (2021) global DWT reconstruction, but with the latter leading by up to 4 kyr.
400 Our results do not provide evidence of the strength of such correlations at shorter timescales, and additional sites that help to increase the temporal resolution would be very beneficial in this respect.

Besides the low resolution and high uncertainty there are some significant weaknesses to address in future work: in particular, dependence on records from distant sites in the North Atlantic, which imposes assumptions on the persistence of ocean circulation patterns during past climate states; and an absence of sites with reconstructions from multiple methods, which prevents
405 one of the most valuable means of validation. Given the importance of the deep ocean in both climate variability and Antarctic Ice Sheet mass balance, an increase in the number of South Atlantic or Southern Ocean sites with BWT reconstructions is urgently needed, for its own worth and also for use by modellers as a boundary condition or for validation.

Data availability. Original temperature reconstructions are available from the sources cited in Table 1. The synthesis is being archived at Pangaea and is also available from the authors on request.

<https://doi.org/10.5194/egusphere-2023-850>

Preprint. Discussion started: 9 May 2023

© Author(s) 2023. CC BY 4.0 License.



410 *Author contributions.* DC compiled the synthesis. Both authors contributed to the manuscript.

Competing interests. The authors declare no competing interests

Acknowledgements. This study was funded by the European Union's Horizon 2020 research and innovation programme under grant agreement no. 820575 (TiPACCs). We gratefully acknowledge the authors of the original temperature reconstructions cited in Table 1, who have made their data publicly available.



Site	Location	Proxy	Modern BWT (°C)	Chronology	Ref
Chain 82-24-4PC	41.7N 32.9W 3427 m	Ostracod (<i>Kirithe</i>) Mg/Ca	2.6	LR04	Cronin et al. (2000)(**)
DSDP 607	41.0S 33.0W 3427 m	$\delta^{18}\text{O}$ (For)	2.5	Raymo (1992)	Bates et al. (2014)
M16772	1.4S 12.0W 3912 m	Foraminiferal (<i>Cibicides</i> <i>wuellerstorfi</i>) Mg/Ca	1.8	LR04	Martin et al. (2002)(***)
ODP 980	55.4N 14.7W 2168 m	Foraminiferal $\delta^{18}\text{O}$	3.5	Shackleton et al. (1990)	Bates et al. (2014)
ODP 1090	42.9S 8.9E 3702 m	Foraminiferal $\delta^{18}\text{O}$	1.6	Hodell et al. (2003)	Bates et al. (2014)
ODP 1094	53.2S 5.1E 2807 m	Foraminiferal (<i>Melonis pompilioides</i>) Mg/Ca	-0.1	LR04	Hasenfratz et al. (2019)
ODP 1123	41.7S 171.5W 3290 m	Foraminiferal (<i>Uvigerina</i> spp.) Mg/Ca	1.6	LR04	Elderfield et al. (2012)(*)

Table 1. Proxy records used for bottom water temperature reconstructions, based on benthic foraminifera (*Cibicides*, *Melonis* and *Uvigerina* spp.) or ostracods (*Kirithe* spp.). LR04 is the Lisiecki and Raymo (2005) global benthic $\delta^{18}\text{O}$ stack. Notes: (*) BWT recalculated here using the Stirpe et al. (2021) calibration for *Uvigerina* spp. Mg/Ca = 0.073T + 0.9. (**) BWT recalculated here using the Farmer et al. (2012) calibration Mg/Ca = 1.13T + 6.42, which has a more appropriate lower temperature limit (-1.7°C) than the original Dwyer et al. (1995) calibration (3°C). (***) BWT recalculated here using the Healey et al. (2008) *C. wuellerstorfi* calibration Mg/Ca = 0.295T + 0.67.



415 References

- Adusumilli, S., Fricker, H. A., Medley, B., Padman, L., and Siegfried, M. R.: Interannual variations in meltwater input to the Southern Ocean from Antarctic ice shelves, *Nat. Geosci.*, 13, 616–620, <https://doi.org/10.1038/s41561-020-0616-z>, 2020.
- Albrecht, T., Winkelmann, R., and Levermann, A.: Glacial-cycle simulations of the Antarctic Ice Sheet with the Parallel Ice Sheet Model (PISM) – Part 1: Boundary conditions and climatic forcing, *Cryosphere*, 14, 599–632, <https://doi.org/10.5194/tc-14-599-2020>, 2020.
- 420 Anderson, D. M.: Attenuation of millennial-scale events by bioturbation in marine sediments, *Paleoceanography*, 16, 352–357, <https://doi.org/10.1029/2000PA000530>, 2001.
- Arias, P., Bellouin, N., Coppola, E., Jones, R., Krinner, G., Marotzke, J., Naik, V., Palmer, M., Plattner, G.-K., Rogelj, J., Rojas, M., Sillmann, J., Storelvmo, T., Thorne, P., Trewin, B., Rao, K. A., Adhikary, B., Allan, R., Armour, K., Bala, G., Barimalala, R., Berger, S., Canadell, J., Cassou, C., Cherchi, A., Collins, W., Collins, W., Connors, S., Corti, S., Cruz, F., Dentener, F., Dereczynski, C., Luca, A. D., Niang, A. D., Doblas-Reyes, F., Dosio, A., Douville, H., Engelbrecht, F., Eyring, V., Fischer, E., Forster, P., Fox-Kemper, B., Fuglested, J., 425 Fyfe, J., Gillett, N., Goldfarb, L., Gorodetskaya, I., Gutierrez, J., Hamdi, R., Hawkins, E., Hewitt, H., Hope, P., Islam, A., Jones, C., Kaufman, D., Kopp, R., Kosaka, Y., Kossin, J., Krakovska, S., Lee, J.-Y., Li, J., Mauritsen, T., Maycock, T., Meinshausen, M., Min, S.-K., Monteiro, P., Ngo-Duc, T., Otto, F., Pinto, I., Pirani, A., Raghavan, K., Ranasinghe, R., Ruane, A., Ruiz, L., Sallée, J.-B., Samset, B., Sathyendranath, S., Seneviratne, S., Sörensson, A., Szopa, S., Takayabu, I., Tréguier, A.-M., van den Hurk, B., Vautard, R., von 430 Schuckmann, K., Zaehle, S., Zhang, X., , and Zickfeld, K.: Technical Summary, in: *Climate Change 2021: The Physical Science Basis. Contribution of Working Group I to the Sixth Assessment Report of the Intergovernmental Panel on Climate Change*, edited by Masson-Delmotte, V., Zhai, P., Pirani, A., Connors, S., Péan, C., Berger, S., Caud, N., Chen, Y., Goldfarb, L., Gomis, M., Huang, M., Leitzell, K., Lonnoy, E., Matthews, J., Maycock, T., Waterfield, T., Yelekçi, O., Yu, R., , and Zhou, B., pp. 33–144, Cambridge University Press, <https://doi.org/10.1017/9781009157896.002>, 2021.
- 435 Assmann, K. M., Darelus, E., Wåhlin, A. K., Kim, T. W., and Lee, S. H.: Warm Circumpolar Deep Water at the Western Getz Ice Shelf Front, *Antarctica, Geophys. Res. Lett.*, 46, 870–878, <https://doi.org/10.1029/2018GL081354>, 2019.
- Ausín, B., Haghipour, N., Wacker, L., Voelker, A. H. L., Hodell, D., Magill, C., Looser, N., Bernasconi, S. M., and Eglinton, T. I.: Radiocarbon Age Offsets Between Two Surface Dwelling Planktonic Foraminifera Species During Abrupt Climate Events in the SW Iberian Margin, *Paleoceanogr. Paleoclimatol.*, 34, 63–78, <https://doi.org/10.1029/2018PA003490>, 2019.
- 440 Bakker, P., Masson-Delmotte, V., Martrat, B., Charbit, S., Renssen, H., Gröger, M., Krebs-Kanzow, U., Lohmann, G., Lunt, D. J., Pfeiffer, M., Phipps, S. J., Prange, M., Ritz, S. P., Schulz, M., Stenni, B., Stone, E. J., and Varma, V.: Temperature trends during the Present and Last Interglacial periods – a multi-model-data comparison, *Quaternary Science Reviews*, 99, 224–243, <https://doi.org/10.1016/j.quascirev.2014.06.031>, 2014.
- Bamber, J. L., Oppenheimer, M., Kopp, R. E., Aspinall, W. P., and Cooke, R. M.: Ice sheet and climate processes driving the uncertainty 445 in projections of future sea level rise: Findings from a structured expert judgement approach., *Earth’s Future*, n/a, e2022EF002772, <https://doi.org/10.1029/2022EF002772>, 2022.
- Barker, S., Greaves, M., and Elderfield, H.: A study of cleaning procedures used for foraminiferal Mg/Ca paleothermometry, *Geochem. Geophys. Geosyst.*, 4, <https://doi.org/10.1029/2003GC000559>, 2003.
- Bates, S. L., Siddall, M., and Waelbroeck, C.: Hydrographic variations in deep ocean temperature over the mid-Pleistocene transition, 450 *Quaternary Science Reviews*, 88, 147–158, <https://doi.org/10.1016/j.quascirev.2014.01.020>, 2014.



- Biddle, L. C., Heywood, K. J., Kaiser, J., and Jenkins, A.: Glacial Meltwater Identification in the Amundsen Sea, *J. Phys. Oceanogr.*, 47, 933–954, <https://doi.org/10.1175/JPO-D-16-0221.1>, 2017.
- Bougamont, M., Hunke, E., and Tulaczyk, S.: Sensitivity of ocean circulation and sea-ice conditions to loss of West Antarctic ice shelves and ice sheet, *J. Glaciol.*, 53, 490–498, <https://doi.org/10.3189/002214307783258440>, 2007.
- 455 Boyle, E. A. and Keigwin, L.: North Atlantic thermohaline circulation during the past 20,000 years linked to high-latitude surface temperature, *Nature*, 330, 35–40, <https://doi.org/10.1038/330035a0>, 1987.
- Broecker, W., Barker, S., Clark, E., Hajdas, I., and Bonani, G.: Anomalous radiocarbon ages for foraminifera shells, *Paleoceanography*, 21, <https://doi.org/10.1029/2005PA001212>, 2006.
- Bronselaer, B., Winton, M., Griffies, S. M., Hurlin, W. J., Rodgers, K. B., Sergienko, O. V., Stouffer, R. J., and Russell, J. L.: Change in
460 future climate due to Antarctic meltwater, *Nature*, 564, 53–58, <https://doi.org/10.1038/s41586-018-0712-z>, 2018.
- Bryan, S. P. and Marchitto, T. M.: Mg/Ca–temperature proxy in benthic foraminifera: New calibrations from the Florida Straits and a hypothesis regarding Mg/Li, *Paleoceanography*, 23, <https://doi.org/10.1029/2007PA001553>, 2008.
- Buckley, M. W. and Marshall, J.: Observations, inferences, and mechanisms of the Atlantic Meridional Overturning Circulation: A review, *Rev. Geophys.*, 54, 5–63, <https://doi.org/10.1002/2015RG000493>, 2016.
- 465 Burgard, C., Jourdain, N. C., Reese, R., Jenkins, A., and Mathiot, P.: An assessment of basal melt parameterisations for Antarctic ice shelves, *Cryosphere*, 16, 4931–4975, <https://doi.org/10.5194/tc-16-4931-2022>, 2022.
- Chadwick, M., Allen, C. S., Sime, L. C., Crosta, X., and Hillenbrand, C.-D.: Reconstructing Antarctic winter sea-ice extent during Marine Isotope Stage 5e, *Clim. Past*, 18, 129–146, <https://doi.org/10.5194/cp-18-129-2022>, 2022.
- Chandler, D. and Langebroek, P.: Southern Ocean sea surface temperature synthesis: Part 1. Evaluation of temperature proxies at glacial-
470 interglacial time scales, *Quaternary Science Reviews*, 271, 107 191, <https://doi.org/10.1016/j.quascirev.2021.107191>, 2021a.
- Chandler, D. and Langebroek, P.: Southern Ocean sea surface temperature synthesis: Part 2. Penultimate glacial and last interglacial, *Quaternary Science Reviews*, 271, 107 190, <https://doi.org/10.1016/j.quascirev.2021.107190>, 2021b.
- Clark, P. U., Archer, D., Pollard, D., Blum, J. D., Rial, J. A., Brovkin, V., Mix, A. C., Pisias, N. G., and Roy, M.: The middle Pleistocene transition: characteristics, mechanisms, and implications for long-term changes in atmospheric pCO₂, *Quaternary Science Reviews*, 25,
475 3150–3184, <https://doi.org/10.1016/j.quascirev.2006.07.008>, 2006.
- Coggon, R. M., Teagle, D. A. H., Smith-Duque, C. E., Alt, J. C., and Cooper, M. J.: Reconstructing Past Seawater Mg/Ca and Sr/Ca from Mid-Ocean Ridge Flank Calcium Carbonate Veins, *Science*, 327, 1114–1117, <https://doi.org/10.1126/science.1182252>, 2010.
- Cronin, T. M., Dwyer, G. S., Baker, P. A., Rodriguez-Lazaro, J., and DeMartino, D. M.: Orbital and suborbital variability in North Atlantic bottom water temperature obtained from deep-sea ostracod Mg/Ca ratios, *Palaeogeogr. Palaeoclimatol. Palaeoecol.*, 162, 45–57,
480 [https://doi.org/10.1016/S0031-0182\(00\)00104-8](https://doi.org/10.1016/S0031-0182(00)00104-8), 2000.
- Cuffey, K. M., Clow, G. D., Steig, E. J., Buizert, C., Fudge, T. J., Koutnik, M., Waddington, E. D., Alley, R. B., and Severinghaus, J. P.: Deglacial temperature history of West Antarctica, *Proc. Natl. Acad. Sci. U.S.A.*, 113, 14 249–14 254, <https://doi.org/10.1073/pnas.1609132113>, 2016.
- Darelius, E., Daae, K., Dundas, V., Fer, I., Hellmer, H. H., Janout, M., Nicholls, K. W., Sallée, J.-B., and Østerhus, S.: Observational evidence
485 for on-shelf heat transport driven by dense water export in the Weddell Sea, *Nat. Commun.*, 14, 1–7, <https://doi.org/10.1038/s41467-023-36580-3>, 2023.
- DeConto, R. M. and Pollard, D.: Contribution of Antarctica to past and future sea-level rise, *Nature*, 531, 591–597, <https://doi.org/10.1038/nature17145>, 2016.



- DeConto, R. M., Pollard, D., Alley, R. B., Velicogna, I., Gasson, E., Gomez, N., Sadai, S., Condron, A., Gilford, D. M., Ashe, E. L.,
490 Kopp, R. E., Li, D., and Dutton, A.: The Paris Climate Agreement and future sea-level rise from Antarctica, *Nature*, 593, 83–89,
<https://doi.org/10.1038/s41586-021-03427-0>, 2021.
- Dezileau, L., Bareille, G., Reyss, J. L., and Lemoine, F.: Evidence for strong sediment redistribution by bottom currents along the southeast
Indian ridge, *Deep Sea Res. Part I*, 47, 1899–1936, [https://doi.org/10.1016/S0967-0637\(00\)00008-X](https://doi.org/10.1016/S0967-0637(00)00008-X), 2000.
- Duplessy, J. C., Shackleton, N. J., Fairbanks, R. G., Labeyrie, L., Oppo, D., and Kallel, N.: Deepwater source varia-
495 tions during the last climatic cycle and their impact on the global deepwater circulation, *Paleoceanography*, 3, 343–360,
<https://doi.org/10.1029/PA003i003p00343>, 1988.
- Dwyer, G. S., Cronin, T. M., Baker, P. A., Raymo, M. E., Buzas, J. S., and Corrège, T.: North Atlantic Deepwater Temperature Change During
Late Pliocene and Late Quaternary Climatic Cycles, *Science*, 270, 1347–1351, <https://doi.org/10.1126/science.270.5240.1347>, 1995.
- Edwards, T. L., Brandon, M. A., Durand, G., Edwards, N. R., Golledge, N. R., Holden, P. B., Nias, I. J., Payne, A. J., Ritz, C., and Wernecke,
500 A.: Revisiting Antarctic ice loss due to marine ice-cliff instability, *Nature*, 566, 58–64, <https://doi.org/10.1038/s41586-019-0901-4>, 2019.
- Elderfield, H., Ferretti, P., Greaves, M., Crowhurst, S., McCave, I. N., Hodell, D., and Piotrowski, A. M.: Evolution of Ocean Temperature
and Ice Volume Through the Mid-Pleistocene Climate Transition, *Science*, 337, 704–709, <https://doi.org/10.1126/science.1221294>, 2012.
- Evans, D. and Müller, W.: Deep time foraminifera Mg/Ca paleothermometry: Nonlinear correction for secular change in seawater Mg/Ca,
Paleoceanography, 27, <https://doi.org/10.1029/2012PA002315>, 2012.
- 505 Farmer, J. R., Cronin, T. M., and Dwyer, G. S.: Ostracode Mg/Ca paleothermometry in the North Atlantic and Arctic oceans: Evaluation of
a carbonate ion effect, *Paleoceanography*, 27, <https://doi.org/10.1029/2012PA002305>, 2012.
- Fox-Kemper, B., Hewitt, H., Xiao, C., Aðalgeirsdóttir, G., Drijfhout, S., Edwards, T., Golledge, N., Hemer, M., Kopp, R., Krinner, G., Mix,
A., Notz, D., Nowicki, S., Nurhati, I., Ruiz, L., Sallée, J.-B., Slangen, A., and Yu, Y.: Ocean, Cryosphere and Sea Level Change, in: *Climate
Change 2021: The Physical Science Basis. Contribution of Working Group I to the Sixth Assessment Report of the Intergovernmental
510 Panel on Climate Change*, edited by Masson-Delmotte, V., Zhai, P., Pirani, A., Connors, S., Péan, C., Berger, S., Caud, N., Chen, Y.,
Goldfarb, L., Gomis, M., Huang, M., Leitzell, K., Lonnoy, E., Matthews, J., Maycock, T., Waterfield, T., Yelekçi, O., Yu, R., and Zhou,
B., Cambridge University Press, UK, 2021.
- Gilford, D. M., Ashe, E. L., DeConto, R. M., Kopp, R. E., Pollard, D., and Rovere, A.: Could the Last Interglacial Con-
strain Projections of Future Antarctic Ice Mass Loss and Sea-Level Rise?, *J. Geophys. Res. Earth Surf.*, 125, e2019JF005418,
515 <https://doi.org/10.1029/2019JF005418>, 2020.
- Gjermundsen, A., Nummelin, A., Olivie, D., Bentsen, M., Seland, Ø., and Schulz, M.: Shutdown of Southern Ocean convection controls
long-term greenhouse gas-induced warming, *Nat. Geosci.*, 14, 724–731, <https://doi.org/10.1038/s41561-021-00825-x>, 2021.
- Goelzer, H., Huybrechts, P., Loutre, M.-F., and Fichefet, T.: Last Interglacial climate and sea-level evolution from a coupled ice sheet–climate
model, *Clim. Past*, 12, 2195–2213, <https://doi.org/10.5194/cp-12-2195-2016>, 2016.
- 520 Golledge, N. R., Clark, P. U., He, F., Dutton, A., Turney, C. S. M., Fogwill, C. J., Naish, T. R., Levy, R. H., McKay, R. M., Lowry, D. P.,
Bertler, N. A. N., Dunbar, G. B., and Carlson, A. E.: Retreat of the Antarctic Ice Sheet During the Last Interglaciation and Implications
for Future Change, *Geophys. Res. Lett.*, 48, e2021GL094513, <https://doi.org/10.1029/2021GL094513>, 2021.
- Gu, S., Liu, Z., Zhang, J., Rempfer, J., Joos, F., and Oppo, D. W.: Coherent Response of Antarctic Intermediate Water and Atlantic Meridional
Overturning Circulation During the Last Deglaciation: Reconciling Contrasting Neodymium Isotope Reconstructions From the Tropical
525 Atlantic, *Paleoceanography*, 32, 1036–1053, <https://doi.org/10.1002/2017PA003092>, 2017.



- Hasenfratz, A. P., Jaccard, S. L., Martínez-García, A., Sigman, D. M., Hodell, D. A., Vance, D., Bernasconi, S. M., Kleiven, H. K. F., Haumann, F. A., and Haug, G. H.: The residence time of Southern Ocean surface waters and the 100,000-year ice age cycle, *Science*, 363, 1080–1084, <https://doi.org/10.1126/science.aat7067>, 2019.
- 530 Healey, S. L., Thunell, R. C., and Corliss, B. H.: The Mg/Ca-temperature relationship of benthic foraminiferal calcite: New core-top calibrations in the <math><4\text{ }^\circ\text{C}</math> temperature range, *Earth Planet. Sci. Lett.*, 272, 523–530, <https://doi.org/10.1016/j.epsl.2008.05.023>, 2008.
- Herraz-Borreguero, L., Coleman, R., Allison, I., Rintoul, S. R., Craven, M., and Williams, G. D.: Circulation of modified Circumpolar Deep Water and basal melt beneath the Amery Ice Shelf, East Antarctica, *J. Geophys. Res. Oceans*, 120, 3098–3112, <https://doi.org/10.1002/2015JC010697>, 2015.
- Hewitt, H. T., Roberts, M., Mathiot, P., Biastoch, A., Blockley, E., Chassignet, E. P., Fox-Kemper, B., Hyder, P., Marshall, D. P., Popova, E., Treguier, A.-M., Zanna, L., Yool, A., Yu, Y., Beadling, R., Bell, M., Kuhlbrodt, T., Arsouze, T., Bellucci, A., Castruccio, F., Gan, B., Putrasahan, D., Roberts, C. D., Van Roekel, L., and Zhang, Q.: Resolving and Parameterising the Ocean Mesoscale in Earth System Models, *Curr. Clim. Change Rep.*, 6, 137–152, <https://doi.org/10.1007/s40641-020-00164-w>, 2020.
- 535 Heywood, K. J., Schmidtko, S., Heuz, C., Kaiser, J., Jickells, T. D., Queste, B. Y., Stevens, D. P., Wadley, M., Thompson, A. F., Fielding, S., Guihen, D., Creed, E., Ridley, J. K., and Smith, W.: Ocean processes at the Antarctic continental slope, *Philos. Trans. Royal Soc. A*, 372, 2013047, <https://doi.org/10.1098/rsta.2013.0047>, 2014.
- 540 Hillenbrand, C.-D., Smith, J. A., Hodell, D. A., Greaves, M., Poole, C. R., Kender, S., Williams, M., Andersen, T. J., Jernas, P. E., Elderfield, H., Klages, J. P., Roberts, S. J., Gohl, K., Larter, R. D., and Kuhn, G.: West Antarctic Ice Sheet retreat driven by Holocene warm water incursions, *Nature*, 547, 43–48, <https://doi.org/10.1038/nature22995>, 2017.
- Hodell, D. A., Venz, K. A., Charles, C. D., and Ninnemann, U. S.: Pleistocene vertical carbon isotope and carbonate gradients in the South Atlantic sector of the Southern Ocean, *Geochem. Geophys. Geosyst.*, 4, 1–19, <https://doi.org/10.1029/2002GC000367>, 2003.
- Hoffman, J. S., Clark, P. U., Parnell, A. C., and He, F.: Regional and global sea-surface temperatures during the last interglaciation, *Science*, 355, 276–279, <https://doi.org/10.1126/science.aai8464>, 2017.
- Johnsen, S. J., Dahl-Jensen, D., Dansgaard, W., and Gundestrup, N.: Greenland palaeotemperatures derived from GRIP bore hole temperature and ice core isotope profiles, *Tellus B: Chem. Phys. Meteorol.*, 47, 624–629, <https://doi.org/10.3402/tellusb.v47i5.16077>, 1995.
- 550 Jouzel, J., Masson-Delmotte, V., Cattani, O., Dreyfus, G., Falourd, S., Hoffmann, G., Minster, B., Nouet, J., Barnola, J. M., Chappellaz, J., Fischer, H., Gallet, J. C., Johnsen, S., Leuenberger, M., Loulergue, L., Luethi, D., Oerter, H., Parrenin, F., Raisbeck, G., Raynaud, D., Schilt, A., Schwander, J., Selmo, E., Souchez, R., Spahni, R., Stauffer, B., Steffensen, J. P., Stenni, B., Stocker, T. F., Tison, J. L., Werner, M., and Wolff, E. W.: Orbital and Millennial Antarctic Climate Variability over the Past 800,000 Years, *Science*, 317, 793–796, <https://doi.org/10.1126/science.1141038>, 2007.
- 555 Kageyama, M., Harrison, S. P., Kapsch, M.-L., Lofverstrom, M., Lora, J. M., Mikolajewicz, U., Sherriff-Tadano, S., Vadsaria, T., Abe-Ouchi, A., Bouttes, N., Chandan, D., Gregoire, L. J., Ivanovic, R. F., Izumi, K., LeGrande, A. N., Lhardy, F., Lohmann, G., Morozova, P. A., Ohgaito, R., Paul, A., Peltier, W. R., Poulsen, C. J., Quiquet, A., Roche, D. M., Shi, X., Tierney, J. E., Valdes, P. J., Volodin, E., and Zhu, J.: The PMIP4 Last Glacial Maximum experiments: preliminary results and comparison with the PMIP3 simulations, *Clim. Past*, 17, 1065–1089, <https://doi.org/10.5194/cp-17-1065-2021>, 2021.
- 560 Kawabe, M. and Fujio, S.: Pacific ocean circulation based on observation, *J. Oceanogr.*, 66, 389–403, <https://doi.org/10.1007/s10872-010-0034-8>, 2010.
- Kim, J., Goldstein, S. L., Pena, L. D., Jaume-Seguí, M., Knudson, K. P., Yehudai, M., and Bolge, L.: North Atlantic Deep Water during Pleistocene interglacials and glacials, *Quaternary Science Reviews*, 269, 107146, <https://doi.org/10.1016/j.quascirev.2021.107146>, 2021.



- Kreuzer, M., Reese, R., Huiskamp, W. N., Petri, S., Albrecht, T., Feulner, G., and Winkelmann, R.: Coupling framework (1.0) for the PISM (1.1.4) ice sheet model and the MOM5 (5.1.0) ocean model via the PICO ice shelf cavity model in an Antarctic domain, *Geosci. Model Dev.*, 14, 3697–3714, <https://doi.org/10.5194/gmd-14-3697-2021>, 2021.
- Legrain, E., Parrenin, F., and Capron, E.: A gradual change is more likely to have caused the Mid-Pleistocene Transition than an abrupt event, *Commun. Earth Environ.*, 4, 1–10, <https://doi.org/10.1038/s43247-023-00754-0>, 2023.
- Lisiecki, L. E. and Raymo, M. E.: A Pliocene-Pleistocene stack of 57 globally distributed benthic $\delta^{18}\text{O}$ records, *Paleoceanography*, 20, <https://doi.org/10.1029/2004PA001071>, 2005.
- Lumpkin, R. and Speer, K.: Global Ocean Meridional Overturning, *J. Phys. Oceanogr.*, 37, 2550–2562, <https://doi.org/10.1175/JPO3130.1>, 2007.
- Lund, D. C., Adkins, J. F., and Ferrari, R.: Abyssal Atlantic circulation during the Last Glacial Maximum: Constraining the ratio between transport and vertical mixing, *Paleoceanography*, 26, <https://doi.org/10.1029/2010PA001938>, 2011.
- MacAyeal, D. R.: Thermohaline circulation below the Ross Ice Shelf: A consequence of tidally induced vertical mixing and basal melting, *J. Geophys. Res. Oceans*, 89, 597–606, <https://doi.org/10.1029/JC089iC01p00597>, 1984.
- Mackie, S., Langhorne, P. J., Heorton, H. D. B. S., Smith, I. J., Feltham, D. L., and Schroeder, D.: Sea Ice Formation in a Coupled Climate Model Including Grease Ice, *J. Adv. Model. Earth Syst.*, 12, e2020MS002103, <https://doi.org/10.1029/2020MS002103>, 2020a.
- Mackie, S., Smith, I. J., Ridley, J. K., Stevens, D. P., and Langhorne, P. J.: Climate Response to Increasing Antarctic Iceberg and Ice Shelf Melt, *J. Clim.*, 33, 8917–8938, <https://doi.org/10.1175/JCLI-D-19-0881.1>, 2020b.
- Marchitto, T. M., Oppo, D. W., and Curry, W. B.: Paired benthic foraminiferal Cd/Ca and Zn/Ca evidence for a greatly increased presence of Southern Ocean Water in the glacial North Atlantic, *Paleoceanography*, 17, 10–1–10–18, <https://doi.org/10.1029/2000PA000598>, 2002.
- Marcott, S. A., Shakun, J. D., Clark, P. U., and Mix, A. C.: A Reconstruction of Regional and Global Temperature for the Past 11,300 Years, *Science*, 339, 1198–1201, <https://doi.org/10.1126/science.1228026>, 2013.
- Marshall, J. and Speer, K.: Closure of the meridional overturning circulation through Southern Ocean upwelling, *Nat. Geosci.*, 5, 171–180, <https://doi.org/10.1038/ngeo1391>, 2012.
- Martin, P. A., Lea, D. W., Rosenthal, Y., Shackleton, N. J., Sarnthein, M., and Papenfuss, T.: Quaternary deep sea temperature histories derived from benthic foraminiferal Mg/Ca, *Earth Planet. Sci. Lett.*, 198, 193–209, [https://doi.org/10.1016/S0012-821X\(02\)00472-7](https://doi.org/10.1016/S0012-821X(02)00472-7), 2002.
- Mawbey, E. M., Hendry, K. R., Greaves, M. J., Hillenbrand, C.-D., Kuhn, G., Spencer-Jones, C. L., McClymont, E. L., Vadman, K. J., Shevenell, A. E., Jernas, P. E., and Smith, J. A.: Mg/Ca-Temperature Calibration of Polar Benthic foraminifera species for reconstruction of bottom water temperatures on the Antarctic shelf, *Geochim. Cosmochim. Acta*, 283, 54–66, <https://doi.org/10.1016/j.gca.2020.05.027>, 2020.
- Mekik, F.: Radiocarbon dating of planktonic foraminifer shells: A cautionary tale, *Paleoceanography*, 29, 13–29, <https://doi.org/10.1002/2013PA002532>, 2014.
- Mercer, J. H.: West Antarctic ice sheet and CO₂ greenhouse effect: a threat of disaster, *Nature*, 271, 321–325, <https://doi.org/10.1038/271321a0>, 1978.
- Mercer, J. H.: Simultaneous Climatic Change in Both Hemispheres and Similar Bipolar Interglacial Warming: Evidence and Implications, in: *Climate Processes and Climate Sensitivity*, pp. 307–313, Wiley, <https://doi.org/10.1029/GM029p0307>, 1984.
- Muglia, J. and Schmittner, A.: Carbon isotope constraints on glacial Atlantic meridional overturning: Strength vs depth, *Quaternary Science Reviews*, 257, 106844, <https://doi.org/10.1016/j.quascirev.2021.106844>, 2021.



- Muschitiello, F., D'Andrea, W. J., Schmittner, A., Heaton, T. J., Balascio, N. L., DeRoberts, N., Caffee, M. W., Woodruff, T. E., Welten, K. C., Skinner, L. C., Simon, M. H., and Dokken, T. M.: Deep-water circulation changes lead North Atlantic climate during deglaciation, *Nat. Commun.*, 10, 1–10, <https://doi.org/10.1038/s41467-019-09237-3>, 2019.
- Naveira Garabato, A. C., Heywood, K. J., and Stevens, D. P.: Modification and pathways of Southern Ocean Deep Waters in the Scotia Sea, *Deep Sea Res. Part I*, 49, 681–705, [https://doi.org/10.1016/S0967-0637\(01\)00071-1](https://doi.org/10.1016/S0967-0637(01)00071-1), 2002.
- Noble, T. L., Rohling, E. J., Aitken, A. R. A., Bostock, H. C., Chase, Z., Gomez, N., Jong, L. M., King, M. A., Mackintosh, A. N., McCormack, F. S., McKay, R. M., Menviel, L., Phipps, S. J., Weber, M. E., Fogwill, C. J., Gayen, B., Golledge, N. R., Gwyther, D. E., Hogg, A. McC., Martos, Y. M., Pena-Molino, B., Roberts, J., van de Flierdt, T., and Williams, T.: The Sensitivity of the Antarctic Ice Sheet to a Changing Climate: Past, Present, and Future, *Rev. Geophys.*, 58, e2019RG000663, <https://doi.org/10.1029/2019RG000663>, 2020.
- 605 Oppo, D. W. and Curry, W. B.: Deep Atlantic Circulation During the Last Glacial Maximum and Deglaciation, *Nature Education Knowledge*, 3, 2012.
- Otto-Bliesner, B. L., Brady, E. C., Zhao, A., Brierley, C. M., Axford, Y., Capron, E., Govin, A., Hoffman, J. S., Isaacs, E., Kageyama, M., Scussolini, P., Tzedakis, P. C., Williams, C. J. R., Wolff, E., Abe-Ouchi, A., Braconnot, P., Ramos Buarque, S., Cao, J., de Vernal, A., Guarino, M. V., Guo, C., LeGrande, A. N., Lohmann, G., Meissner, K. J., Menviel, L., Morozova, P. A., Nisancioglu, K. H., O'ishi, R., Salas y Mélia, D., Shi, X., Sicard, M., Sime, L., Stepanek, C., Tomas, R., Volodin, E., Yeung, N. K. H., Zhang, Q., Zhang, Z., and Zheng, W.: Large-scale features of Last Interglacial climate: results from evaluating the lig127k simulations for the Coupled Model Intercomparison Project (CMIP6)–Paleoclimate Modeling Intercomparison Project (PMIP4), *Clim. Past*, 17, 63–94, <https://doi.org/10.5194/cp-17-63-2021>, 2021.
- 615 Pardo, P. C., Pérez, F. F., Velo, A., and Gilcoto, M.: Water masses distribution in the Southern Ocean: Improvement of an extended OMP (eOMP) analysis, *Prog. Oceanogr.*, 103, 92–105, <https://doi.org/10.1016/j.pocean.2012.06.002>, 2012.
- Parrenin, F., Masson-Delmotte, V., Köhler, P., Raynaud, D., Paillard, D., Schwander, J., Barbante, C., Landais, A., Wegner, A., and Jouzel, J.: Synchronous Change of Atmospheric CO₂ and Antarctic Temperature During the Last Deglacial Warming, *Science*, 339, 1060–1063, <https://doi.org/10.1126/science.1226368>, 2013.
- Past Interglacials Working Group of PAGES: Interglacials of the last 800,000 years, *Rev. Geophys.*, 54, 162–219, <https://doi.org/10.1002/2015RG000482>, 2016.
- 625 Pelletier, C., Fichefet, T., Goosse, H., Haubner, K., Helsen, S., Huot, P.-V., Kittel, C., Klein, F., Le clec'h, S., van Lipzig, N. P. M., Marchi, S., Massonnet, F., Mathiot, P., Moravceji, E., Moreno-Chamarro, E., Ortega, P., Pattyn, F., Souverijns, N., Van Achter, G., Vanden Broucke, S., Vanhulle, A., Verfaillie, D., and Zipf, L.: PARASO, a circum-Antarctic fully coupled ice-sheet–ocean–sea-ice–atmosphere–land model involving f.ETISH1.7, NEMO3.6, LIM3.6, COSMO5.0 and CLM4.5, *Geosci. Model Dev.*, 15, 553–594, <https://doi.org/10.5194/gmd-15-553-2022>, 2022.
- 630 Petty, A. A., Feltham, D. L., and Holland, P. R.: Impact of Atmospheric Forcing on Antarctic Continental Shelf Water Masses, *J. Phys. Oceanogr.*, 43, 920–940, <https://doi.org/10.1175/JPO-D-12-0172.1>, 2013.
- Piasecki, A., Bernasconi, S. M., Grauel, A.-L., Hannisdal, B., Ho, S. L., Leutert, T. J., Marchitto, T. M., Meinicke, N., Tisserand, A., and Meckler, N.: Application of Clumped Isotope Thermometry to Benthic Foraminifera, *Geochem. Geophys. Geosyst.*, 20, 2082–2090, <https://doi.org/10.1029/2018GC007961>, 2019.
- 635 Pollard, D. and DeConto, R. M.: Description of a hybrid ice sheet-shelf model, and application to Antarctica, *Geosci. Model Dev.*, 5, 1273–1295, <https://doi.org/10.5194/gmd-5-1273-2012>, 2012.



- Purich, A. and England, M. H.: Historical and Future Projected Warming of Antarctic Shelf Bottom Water in CMIP6 Models, *Geophys. Res. Lett.*, 48, e2021GL092752, <https://doi.org/10.1029/2021GL092752>, 2021.
- 640 Rahmstorf, S.: Rapid climate transitions in a coupled ocean–atmosphere model, *Nature*, 372, 82–85, <https://doi.org/10.1038/372082a0>, 1994.
- Raitzsch, M., Kuhnert, H., Groeneveld, J., and Bickert, T.: Benthic foraminifer Mg/Ca anomalies in South Atlantic core top sediments and their implications for paleothermometry, *Geochem. Geophys. Geosyst.*, 9, <https://doi.org/10.1029/2007GC001788>, 2008.
- Raymo, M. E.: Global Climate Change: A Three Million Year Perspective, in: *Start of a Glacial*, pp. 207–223, Springer, Berlin, Germany, https://doi.org/10.1007/978-3-642-76954-2_15, 1992.
- 645 Raymo, M. E., Ruddiman, W. F., Shackleton, N. J., and Oppo, D. W.: Evolution of Atlantic-Pacific $\delta^{13}\text{C}$ gradients over the last 2.5 m.y., *Earth Planet. Sci. Lett.*, 97, 353–368, [https://doi.org/10.1016/0012-821X\(90\)90051-X](https://doi.org/10.1016/0012-821X(90)90051-X), 1990.
- Reese, R., Albrecht, T., Mengel, M., Asay-Davis, X., and Winkelmann, R.: Antarctic sub-shelf melt rates via PICO, *Cryosphere*, 12, 1969–1985, <https://doi.org/10.5194/tc-12-1969-2018>, 2018.
- Rhein, M., Kieke, D., and Steinfeldt, R.: Advection of North Atlantic Deep Water from the Labrador Sea to the southern hemisphere, *J. Geophys. Res. Oceans*, 120, 2471–2487, <https://doi.org/10.1002/2014JC010605>, 2015.
- 650 Ries, J. B.: Review: geological and experimental evidence for secular variation in seawater Mg/Ca (calcite-aragonite seas) and its effects on marine biological calcification, *Biogeosciences*, 7, 2795–2849, <https://doi.org/10.5194/bg-7-2795-2010>, 2010.
- Rintoul, S. R.: The global influence of localized dynamics in the Southern Ocean, *Nature*, 558, 209–218, <https://doi.org/10.1038/s41586-018-0182-3>, 2018.
- 655 Roberts, J., Gottschalk, J., Skinner, L. C., Peck, V. L., Kender, S., Elderfield, H., Waelbroeck, C., Vázquez Riveiros, N., and Hodell, D. A.: Evolution of South Atlantic density and chemical stratification across the last deglaciation, *Proc. Natl. Acad. Sci. U.S.A.*, 113, 514–519, <https://doi.org/10.1073/pnas.1511252113>, 2016.
- Rohling, E. J., Yu, J., Heslop, D., Foster, G. L., Opdyke, B., and Roberts, A. P.: Sea level and deep-sea temperature reconstructions suggest quasi-stable states and critical transitions over the past 40 million years, *Sci. Adv.*, 7, eabf5326, <https://doi.org/10.1126/sciadv.abf5326>, 2021.
- 660 Scherer, R. P.: Quaternary and Tertiary microfossils from beneath Ice Stream B: Evidence for a dynamic West Antarctic Ice Sheet history, *Global Planet. Change*, 4, 395–412, [https://doi.org/10.1016/0921-8181\(91\)90005-H](https://doi.org/10.1016/0921-8181(91)90005-H), 1991.
- Sexton, P. F., Wilson, P. A., and Pearson, P. N.: Microstructural and geochemical perspectives on planktic foraminiferal preservation: “Glassy” versus “Frosty”, *Geochem. Geophys. Geosyst.*, 7, <https://doi.org/10.1029/2006GC001291>, 2006.
- 665 Shackleton, N. J., Berger, A., and Peltier, W. R.: An alternative astronomical calibration of the lower Pleistocene timescale based on ODP Site 677, *Earth Environ. Sci. Trans. R. Soc. Edinburgh*, 81, 251–261, <https://doi.org/10.1017/S0263593300020782>, 1990.
- Shackleton, S., Baggenstos, D., Menking, J. A., Dyonisius, M. N., Bereiter, B., Bauska, T. K., Rhodes, R. H., Brook, E. J., Petrenko, V. V., McConnell, J. R., Kellerhals, T., Häberli, M., Schmitt, J., Fischer, H., and Severinghaus, J. P.: Global ocean heat content in the Last Interglacial, *Nat. Geosci.*, 13, 77–81, <https://doi.org/10.1038/s41561-019-0498-0>, 2020.
- 670 Shakun, J. D., Lea, D. W., Lisiecki, L. E., and Raymo, M. E.: An 800-kyr record of global surface ocean $\delta^{18}\text{O}$ and implications for ice volume-temperature coupling, *Earth Planet. Sci. Lett.*, 426, 58–68, <https://doi.org/10.1016/j.epsl.2015.05.042>, 2015.
- Siahaan, A., Smith, R. S., Holland, P. R., Jenkins, A., Gregory, J. M., Lee, V., Mathiot, P., Payne, A. J. x.-z., Ridley, J. K. x.-z., and Jones, C. G.: The Antarctic contribution to 21st-century sea-level rise predicted by the UK Earth System Model with an interactive ice sheet, *Cryosphere*, 16, 4053–4086, <https://doi.org/10.5194/tc-16-4053-2022>, 2022.



- 675 Siddall, M., Hönisch, B., Waelbroeck, C., and Huybers, P.: Changes in deep Pacific temperature during the mid-Pleistocene transition and Quaternary, *Quaternary Science Reviews*, 29, 170–181, <https://doi.org/10.1016/j.quascirev.2009.05.011>, 2010.
- Silvano, A., Rintoul, S. R., Peña-Molino, B., and Williams, G. D.: Distribution of water masses and meltwater on the continental shelf near the Totten and Moscow University ice shelves, *J. Geophys. Res. Oceans*, 122, 2050–2068, <https://doi.org/10.1002/2016JC012115>, 2017.
- Sloyan, B. M. and Rintoul, S. R.: The Southern Ocean Limb of the Global Deep Overturning Circulation, *J. Phys. Oceanogr.*, 31, 143–173, [https://doi.org/10.1175/1520-0485\(2001\)031<0143:TSOLOT>2.0.CO;2](https://doi.org/10.1175/1520-0485(2001)031<0143:TSOLOT>2.0.CO;2), 2001.
- 680 Smethie, W. M., Fine, R. A., Putzka, A., and Jones, E. P.: Tracing the flow of North Atlantic Deep Water using chlorofluorocarbons, *J. Geophys. Res. Oceans*, 105, 14 297–14 323, <https://doi.org/10.1029/1999JC900274>, 2000.
- Stewart, A. L. and Thompson, A. F.: Eddy-mediated transport of warm Circumpolar Deep Water across the Antarctic Shelf Break, *Geophys. Res. Lett.*, 42, 432–440, <https://doi.org/10.1002/2014GL062281>, 2015.
- 685 Stirpe, C. R., Allen, K. A., Sikes, E. L., Zhou, X., Rosenthal, Y., Cruz-Uribe, A. M., and Brooks, H. L.: The Mg/Ca proxy for temperature: A *Uvigerina* Core-Top Study in the Southwest Pacific, *Geochim. Cosmochim. Acta*, <https://doi.org/10.1016/j.gca.2021.06.015>, 2021.
- Sun, S., Eisenman, I., Zanna, L., and Stewart, A. L.: Surface Constraints on the Depth of the Atlantic Meridional Overturning Circulation: Southern Ocean versus North Atlantic, *J. Clim.*, 33, 3125–3149, <https://doi.org/10.1175/JCLI-D-19-0546.1>, 2020.
- Sutter, J., Fischer, H., Grosfeld, K., Karlsson, N. B., Kleiner, T., Van Liefferinge, B., and Eisen, O.: Modelling the Antarctic Ice Sheet across the mid-Pleistocene transition – implications for Oldest Ice, *Cryosphere*, 13, 2023–2041, <https://doi.org/10.5194/tc-13-2023-2019>, 2019.
- 690 Talley, L. D.: Closure of the Global Overturning Circulation Through the Indian, Pacific, and Southern Oceans: Schematics and Transports, *Oceanography*, 26, <https://doi.org/10.5670/oceanog.2013.07>, 2013.
- Tamsitt, V., Drake, H. F., Morrison, A. K., Talley, L. D., Dufour, C. O., Gray, A. R., Griffies, S. M., Mazloff, M. R., Sarmiento, J. L., Wang, J., and Weijer, W.: Spiraling pathways of global deep waters to the surface of the Southern Ocean, *Nat. Commun.*, 8, 1–10, <https://doi.org/10.1038/s41467-017-00197-0>, 2017.
- 695 Tamsitt, V., England, M. H., Rintoul, S. R., and Morrison, A. K.: Residence Time and Transformation of Warm Circumpolar Deep Water on the Antarctic Continental Shelf, *Geophys. Res. Lett.*, 48, e2021GL096092, <https://doi.org/10.1029/2021GL096092>, 2021.
- Thompson, A. F., Stewart, A. L., and Bischoff, T.: A Multibasin Residual-Mean Model for the Global Overturning Circulation, *J. Phys. Oceanogr.*, 46, 2583–2604, <https://doi.org/10.1175/JPO-D-15-0204.1>, 2016.
- 700 Tigchelaar, M., Timmermann, A., Pollard, D., Friedrich, T., and Heinemann, M.: Local insolation changes enhance Antarctic interglacials: Insights from an 800,000-year ice sheet simulation with transient climate forcing, *Earth Planet. Sci. Lett.*, 495, 69–78, <https://doi.org/10.1016/j.epsl.2018.05.004>, 2018.
- Tisserand, A. A., Dokken, T. M., Waelbroeck, C., Gherardi, J.-M., Scao, V., Fontanier, C., and Jorissen, F.: Refining benthic foraminiferal Mg/Ca-temperature calibrations using core-tops from the western tropical Atlantic: Implication for paleotemperature estimation, *Geochem. Geophys. Geosyst.*, 14, 929–946, <https://doi.org/10.1002/ggge.20043>, 2013.
- 705 Totten, R. L., Majewski, W., Anderson, J. B., Yokoyama, Y., Fernandez, R., and Jakobsson, M.: Oceanographic influences on the stability of the Cosgrove Ice Shelf, Antarctica, *Holocene*, 27, 1645–1658, <https://doi.org/10.1177/0959683617702226>, 2017.
- Tripathi, A. K., Eagle, R. A., Thiagarajan, N., Gagnon, A. C., Bauch, H., Halloran, P. R., and Eiler, J. M.: 13C–18O isotope signatures and ‘clumped isotope’ thermometry in foraminifera and coccoliths, *Geochim. Cosmochim. Acta*, 74, 5697–5717, <https://doi.org/10.1016/j.gca.2010.07.006>, 2010.
- 710



- Turney, C. S. M., Jones, R. T., McKay, N. P., van Sebille, E., Thomas, Z. A., Hillenbrand, C.-D., and Fogwill, C. J.: A global mean sea surface temperature dataset for the Last Interglacial (129–116 ka) and contribution of thermal expansion to sea level change, *Earth Syst. Sci. Data*, 12, 3341–3356, <https://doi.org/10.5194/essd-12-3341-2020>, 2020.
- 715 Tzedakis, P. C., Raynaud, D., McManus, J. F., Berger, A., Brovkin, V., and Kiefer, T.: Interglacial diversity, *Nat. Geosci.*, 2, 751–755, <https://doi.org/10.1038/ngeo660>, 2009.
- van Wijk, E. M., Rintoul, S. R., Wallace, L. O., Ribeiro, N., and Herraiz-Borreguero, L.: Vulnerability of Denman Glacier to Ocean Heat Flux Revealed by Profiling Float Observations, *Geophys. Res. Lett.*, 49, e2022GL100460, <https://doi.org/10.1029/2022GL100460>, 2022.
- Vaughan, D. G., Barnes, D. K. A., Fretwell, P. T., and Bingham, R. G.: Potential seaways across West Antarctica, *Geochem. Geophys. Geosyst.*, 12, <https://doi.org/10.1029/2011GC003688>, 2011.
- 720 Waelbroeck, C., Labeyrie, L., Michel, E., Duplessy, J. C., McManus, J. F., Lambeck, K., Balbon, E., and Labracherie, M.: Sea-level and deep water temperature changes derived from benthic foraminifera isotopic records, *Quaternary Science Reviews*, 21, 295–305, [https://doi.org/10.1016/S0277-3791\(01\)00101-9](https://doi.org/10.1016/S0277-3791(01)00101-9), 2002.
- Wählin, A. K., Yuan, X., Björk, G., and Nohr, C.: Inflow of Warm Circumpolar Deep Water in the Central Amundsen Shelf, *J. Phys. Oceanogr.*, 40, 1427–1434, <https://doi.org/10.1175/2010JPO4431.1>, 2010.
- 725 Walker, D. P., Brandon, M. A., Jenkins, A., Allen, J. T., Dowdeswell, J. A., and Evans, J.: Oceanic heat transport onto the Amundsen Sea shelf through a submarine glacial trough, *Geophys. Res. Lett.*, 34, <https://doi.org/10.1029/2006GL028154>, 2007.
- Williams, T. J., Martin, E. E., Sikes, E., Starr, A., Umling, N. E., and Glaubke, R.: Neodymium isotope evidence for coupled Southern Ocean circulation and Antarctic climate throughout the last 118,000 years, *Quaternary Science Reviews*, 260, 106915, <https://doi.org/10.1016/j.quascirev.2021.106915>, 2021.
- 730 Yin, Q. and Berger, A.: Interglacial analogues of the Holocene and its natural near future, *Quaternary Science Reviews*, 120, 28–46, <https://doi.org/10.1016/j.quascirev.2015.04.008>, 2015.
- Yu, E.-F., Francois, R., and Bacon, M. P.: Similar rates of modern and last-glacial ocean thermohaline circulation inferred from radiochemical data, *Nature*, 379, 689–694, <https://doi.org/10.1038/379689a0>, 1996.
- Yu, J. and Elderfield, H.: Mg/Ca in the benthic foraminifera *Cibicides wuellerstorfi* and *Cibicides mundulus*: Temperature versus carbonate ion saturation, *Earth Planet. Sci. Lett.*, 276, 129–139, <https://doi.org/10.1016/j.epsl.2008.09.015>, 2008.
- 735 Yu, J., Elderfield, H., Greaves, M., and Day, J.: Preferential dissolution of benthic foraminiferal calcite during laboratory reductive cleaning, *Geochem. Geophys. Geosyst.*, 8, <https://doi.org/10.1029/2006GC001571>, 2007.
- Yu, J., Elderfield, H., and Piotrowski, A. M.: Seawater carbonate ion- $\delta^{13}\text{C}$ systematics and application to glacial–interglacial North Atlantic ocean circulation, *Earth Planet. Sci. Lett.*, 271, 209–220, <https://doi.org/10.1016/j.epsl.2008.04.010>, 2008.
- 740 Zhang, Z., Jansen, E., Sobolowski, S. P., Otterå, O. H., Ramstein, G., Guo, C., Nummelin, A., Bentsen, M., Dong, C., Wang, X., Wang, H., and Guo, Z.: Atmospheric and oceanic circulation altered by global mean sea-level rise, *Nat. Geosci.*, pp. 1–7, <https://doi.org/10.1038/s41561-023-01153-y>, 2023.